



1,2,4-Triazolo[1,5-*a*]pyrimidines: Efficient one-step synthesis and functionalization as influenza polymerase PA-PB1 interaction disruptors



Maria Chiara Pismataro ^{a,1}, Tommaso Felicetti ^{a,1}, Chiara Bertagnin ^b, Maria Giulia Nizi ^a, Anna Bonomini ^b, Maria Letizia Barreca ^a, Violetta Cecchetti ^a, Dirk Jochmans ^c, Steven De Jonghe ^c, Johan Neyts ^c, Arianna Loregian ^b, Oriana Tabarrini ^a, Serena Massari ^{a,*}

^a Department of Pharmaceutical Sciences, University of Perugia, Via Del Liceo 1, 06123, Perugia, Italy

^b Department of Molecular Medicine, University of Padua, Via Gabelli 63, 35121, Padua, Italy

^c KU Leuven, Department of Microbiology, Immunology and Transplantation, Rega Institute for Medical Research, Laboratory of Virology and Chemotherapy, Herestraat 49, Box 1043, 3000, Leuven, Belgium

ARTICLE INFO

Article history:

Received 9 February 2021

Received in revised form

30 March 2021

Accepted 18 April 2021

Available online 26 April 2021

Keywords:

1,2,4-triazolo[1,5-*a*]pyrimidines

Antiviral agents

Influenza virus

SARS-CoV-2

Protein-protein interaction

Influenza polymerase

PA-PB1 interaction

ABSTRACT

In the search for new anti-influenza virus (IV) compounds, we have identified the 1,2,4-triazolo[1,5-*a*]pyrimidine (TZP) as a very suitable scaffold to obtain compounds able to disrupt IV RNA-dependent RNA polymerase (RdRP) PA-PB1 subunits heterodimerization. In this work, in order to acquire further SAR insights for this class of compounds and identify more potent derivatives, we designed and synthesized additional series of analogues to investigate the role of the substituents around the TZP core. To this aim, we developed four facile and efficient one-step procedures for the synthesis of 5-phenyl-, 6-phenyl- and 7-phenyl-2-amino-[1,2,4]triazolo[1,5-*a*]pyrimidines, and 2-amino-5-phenyl-[1,2,4]triazolo[1,5-*a*]pyrimidin-7-ol. Two analogues having the ethyl carboxylate moiety at the C-2 position of the TZP were also prepared in good yields. Then, the scaffolds herein synthesized and two previous scaffolds were functionalized and evaluated for their anti-IAV activity, leading to the identification of compound **22** that showed both anti-PA-PB1 (IC₅₀ = 19.5 μM) and anti-IAV activity (EC₅₀ = 16 μM) at non-toxic concentrations, thus resulting among the most active TZP derivatives reported to date by us. A selection of the synthesized compounds, along with a set of in-house available analogues, was also tested against SARS-CoV-2. The most promising compound **49** from this series displayed an EC₅₀ value of 34.47 μM, highlighting the potential of the TPZ scaffold in the search for anti-CoV agents.

© 2021 Elsevier Masson SAS. All rights reserved.

1. Introduction

Among the four influenza virus (IV) types A, B, C and D, IAV and IBV pose a severe threat for human health, circulating among humans and causing seasonal epidemics. Moreover, pandemic outbreaks can occur if highly virulent and pathogenic IAV strains, deriving from antigenic shift, cross the species barrier and spread easily among human beings that are naïve to the novel strain.

During pandemic events, since long time is needed to produce a new vaccine, antivirals are an important weapon. To date, the antiviral armamentarium to treat IV infections is limited to a few licensed drugs belonging to M2 ion channel inhibitors, which are no longer recommended [1,2], and NA inhibitors [3], towards which, however, many IAV strains developed resistance and IBV showed reduced sensitivity.

Searching for new anti-IV drugs, the viral RNA-dependent RNA polymerase (RdRP) is a really attractive drug target since i) it plays a key role in the biological processes of virus transcription, replication, and evolution [4,5], ii) its structure is highly conserved among IAV, IBV, and ICV strains, and iii) no homologue has been found in mammalian cells. Regarding its structure, RdRP is a heterotrimeric

* Corresponding author. Department of Pharmaceutical Sciences, University of Perugia, 06123, Perugia, Italy.

E-mail address: serena.massari@unipg.it (S. Massari).

¹ Co-first authors.

complex formed by the viral polymerase basic protein 1 (PB1), polymerase basic protein 2 (PB2), and polymerase acidic protein (PA) [6–9]. To date, three compounds targeting each of the three polymerase subunits have been recently approved or in clinical trials: the nucleoside analog **favipiravir** (T-705, Avigan®) [10,11] approved in 2014 in Japan, the PA endonuclease inhibitor **baloxavir marboxil** (Xofluxe™) [12,13] approved in 2018 in both Japan and the USA, and the PB2 cap-binding inhibitor **pimodivir** (VX-787, JNJ-63623872) [14,15] that was recently halted after phase 3 evaluation [16].

In the search for new RdRP inhibitors, we pursued the approach to interfere with the correct assembly of the RdRP subunits by developing protein-protein interaction (PPI) inhibitors. In particular, we focused our attention on the identification of small molecules as disruptors of RdRP PA-PB1 complex formation [17–19]. Compounds that interfere with PA-PB1 interaction have two major advantages over other classes of anti-IV compounds [20,21]. First, residues of both PB1 and PA that are crucial for subunits interaction are highly conserved among IAV strains [22], suggesting that PA-PB1 interaction inhibitors are expected to show broad-spectrum antiviral activity against several human and animal IAV strains, including new pandemic strains. Moreover, IVs showed a limited ability to compensate for mutations deliberately introduced into the PA_C or PB1_N termini [23], thus PA-PB1 inhibitors should be less prone to drug resistance, overcoming the main limitation that characterizes the majority of antiviral drugs.

Our previous studies on the discovery of PA-PB1 inhibitors focused on the optimization of hit compound **1** (Fig. 1), identified by a virtual screening on the PA_C crystal structure [17]. Aromatization of the [1,2,4]triazolo[1,5-*a*]pyrimidine (TZP) core as well as inversion of the C-5/C-7 substituents led to the identification of derivative **2** (Fig. 1) [19], which showed an improved ability to inhibit PA-PB1 interaction and, above all, acquired anti-IV activity at non-toxic concentrations. The inversion of amide bond allowed the functionalization of the C-2 position of the TZP scaffold affording

carbamoyl derivative **3** [24,25] as well as hybrid molecules **4** and **5** (Fig. 1) [19] born by merging the TPZ core with the cycloheptathiophene-3-carboxamide moiety, which showed the best anti-PA-PB1 and anti-IV activity.

The synthesis of the above anti-IV TZPs required the preparation of 2-amino-[1,2,4]triazolo[1,5-*a*]pyrimidine and ethyl [1,2,4]triazolo[1,5-*a*]pyrimidine-2-carboxylate intermediates unsymmetrically substituted at the C-5 and C-7 positions. Since their synthesis was scarcely explored, we were also interested in developing suitable procedures for their preparation. In particular, we recently reported two facile and efficient one-step procedures for the regioselective synthesis of 2-amino-5-methyl-7-phenyl-[1,2,4]triazolo[1,5-*a*]pyrimidine (**6**) and its isomer 2-amino-7-methyl-5-phenyl-[1,2,4]triazolo[1,5-*a*]pyrimidine (**7**) [25] (Fig. 2).

TZP is a privileged structure in chemistry and an important scaffold in medicinal chemistry, mimicking a wide range of natural building blocks and exhibiting different interesting biological activities. A number of biologically active compounds based on the TZP structure has been reported [26,27], such as CNS agents, antihistaminic, anticancer, anti-inflammatory, cardiovascular agents, adenosine receptor antagonists, diuretics, anxiolytic agents, platelet aggregation inhibitors, anxiolytic agents, bronchodilators, antimicrobials, antimalarial, and antiviral. Focusing on antiviral TZP-based compounds, they have been developed against different viruses [28], such as HIV, HCV, HBV, HSV, Chikungunya virus, DENV and IV.

Continuing our search for anti-IV compounds based on innovative TZP cores, in this work, we determined the best reaction conditions for the synthesis of 2-amino-7-phenyl-[1,2,4]triazolo[1,5-*a*]pyrimidine (**8**), 2-amino-5-phenyl-[1,2,4]triazolo[1,5-*a*]pyrimidine (**9**), 2-amino-6-phenyl-[1,2,4]triazolo[1,5-*a*]pyrimidine (**10**) and 2-amino-5-phenyl-[1,2,4]triazolo[1,5-*a*]pyrimidin-7-ol (**11**) (Fig. 2). Analogously to the previously reported C-2 ethyl carboxylate analogues **12** and **13** [25], attempts to synthesize compounds **14–17** (Fig. 2) were also done, successfully providing compounds **14** and **16**.

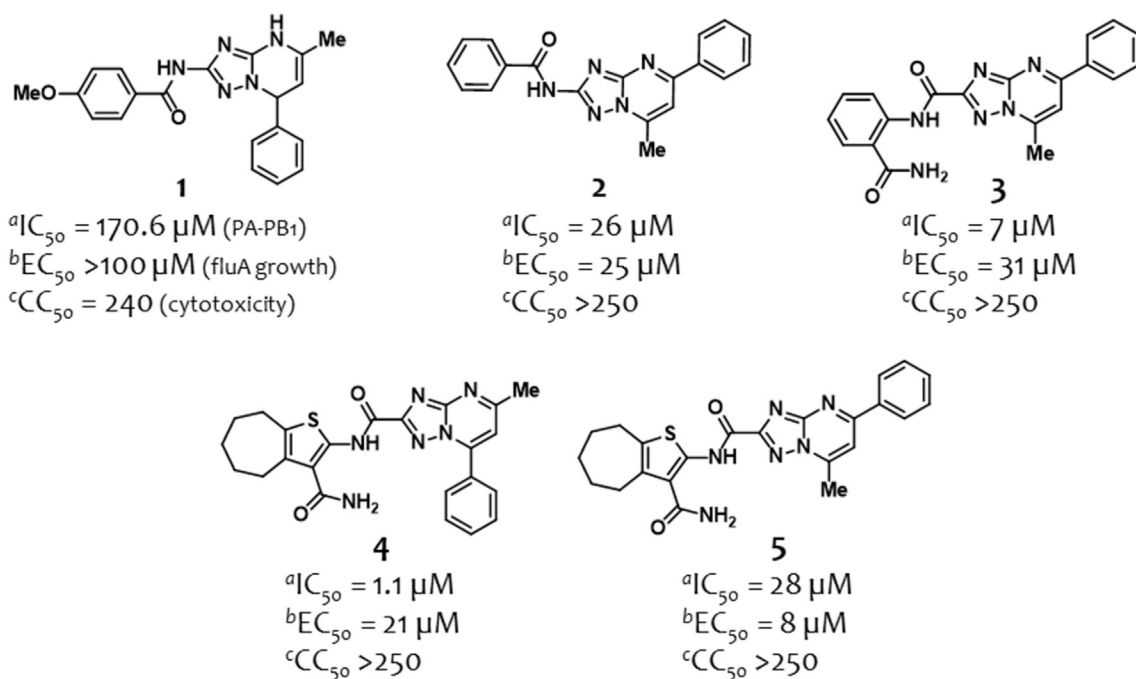


Fig. 1. Examples of [1,2,4]triazolo[1,5-*a*]pyrimidine-based compounds showing anti-PA-PB1 and anti-IV activity. ^a The IC₅₀ value represents the compound concentration that reduces the PA-PB1 complex formation by 50% (ELISA assay); ^b the EC₅₀ value represents the compound concentration that inhibits 50% of IAV replication (PRA assay); ^c the CC₅₀ value represents the compound concentration that inhibits 50% of cell viability (MTT assay).

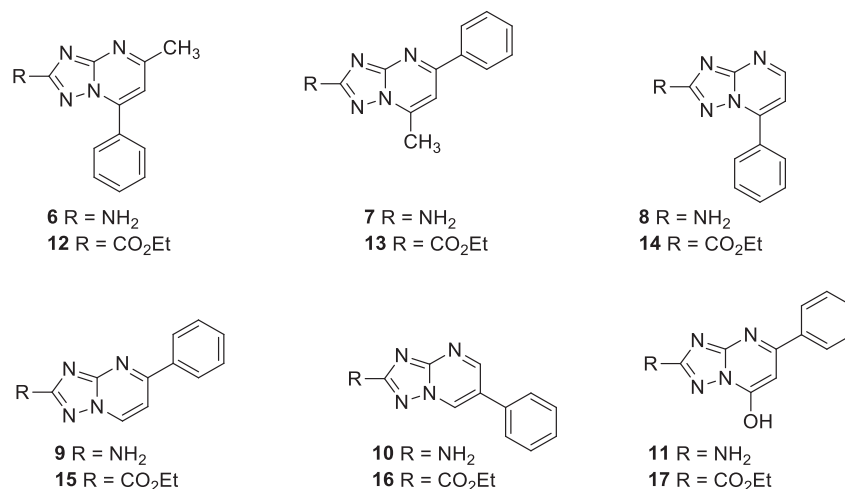


Fig. 2. Structures of 1,2,4-triazolo[1,5-*a*]pyrimidines variously functionalized at the C-5, C-6 and C-7 positions useful for the synthesis of IV RdRP PA-PB1 inhibitors.

Then, scaffolds **8–14** and **16** were used for the preparation of PA-PB1 inhibitors. In particular, three set of compounds (Fig. 3) were synthesized and evaluated for their ability to inhibit the PA-PB1 interaction and IAV replication, with the aim to study the role of the substituent at the C-2, C-5, C-6 and C-7 positions of the TZP core. Additionally, some compounds herein reported, along with a small set of in-house TZP compounds, were evaluated for the anti-SARS-CoV-2 activity.

2. Results and discussion

2.1. Synthesis of 2-amino-[1,2,4]triazolo[1,5-*a*]pyrimidines

Focusing the attention on the synthesis of isomer 2-amino-7-phenyl-[1,2,4]triazolo[1,5-*a*]pyrimidine (**8**), we found that its

regioselective synthesis was reported in literature *via* reaction of 3,5-diamonotriazole (**32**) with 3-(dimethylamino)-1-phenyl-2-propen-1-one (**33**) both in glacial acetic acid at reflux (72% yield) [29] and in EtOH at reflux (100% yield) [30] (Scheme 1a).

Therefore, we initially repeated the reaction in both the solvents and, for this purpose, compound **33** [31] was synthesized as reported in literature, *via* reaction of acetophenone with dimethylformamide dimethyl acetal at 160 °C for 15 min in a microwave oven. In agreement with Ribeiro et al. [29], the reaction in glacial acetic acid at reflux (entry 1, Table 1) furnished **8** in 72% yield. On the other hand, differently from Menet et al. [30], the reaction in EtOH at reflux (entry 2) did not finish after 24 h (also waiting until 48h) furnishing **8** only in 42% yield.

Based on these results, we repeated the reaction in glacial acetic acid using 2 equiv. of **32** (entry 3) and we found that the reaction

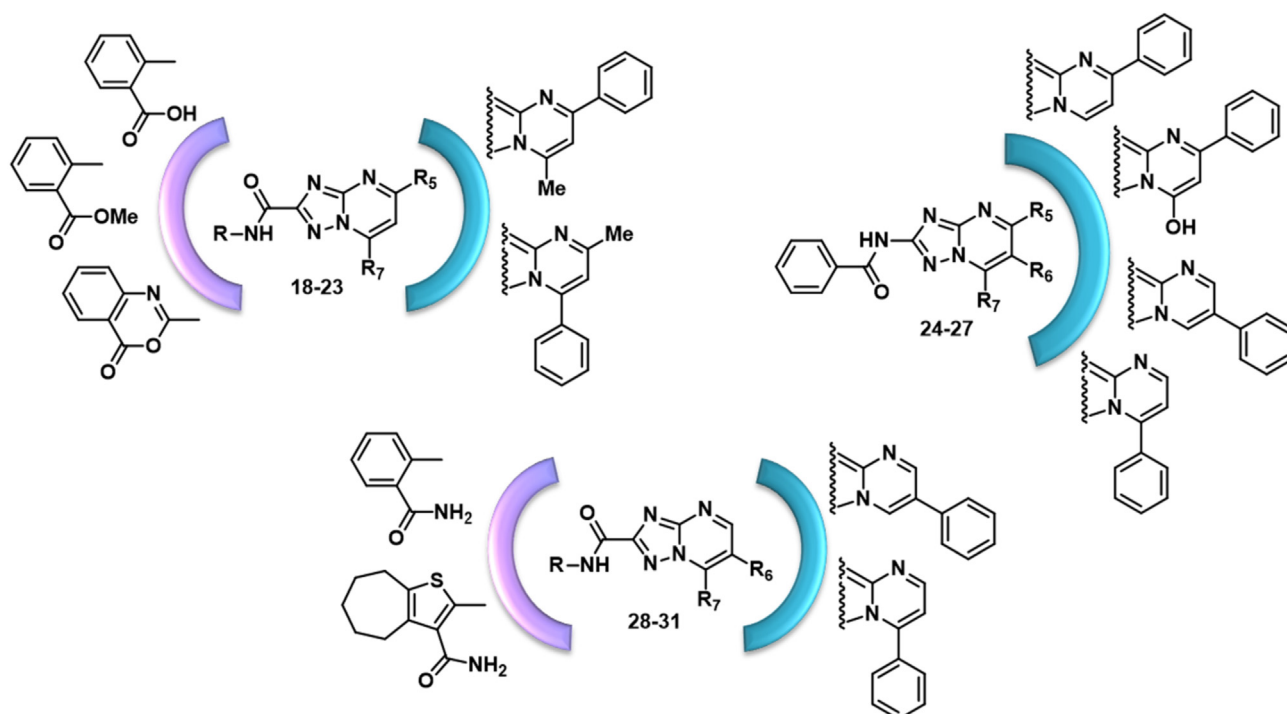
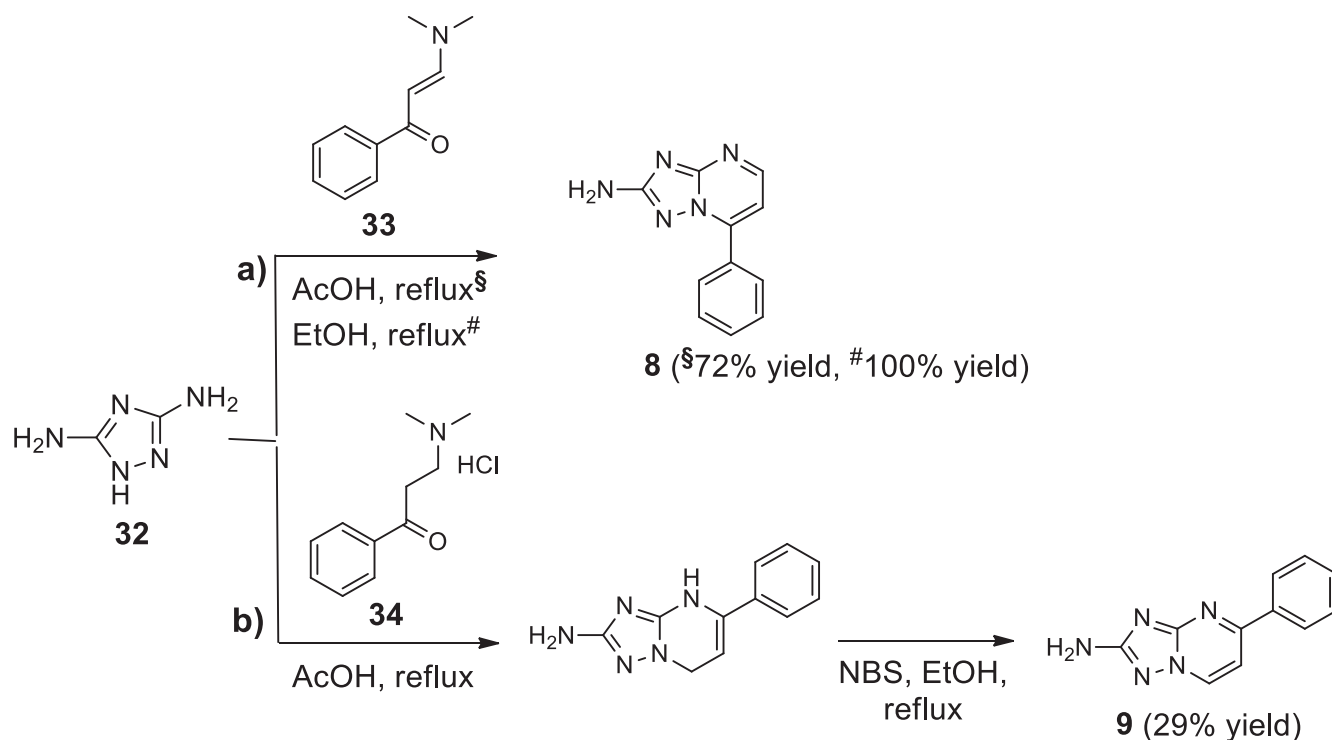


Fig. 3. Structure of the compounds **18–31** designed, synthesized and evaluated as inhibitors of PA-PB1 binding and IAV replication.



Scheme 1. Known procedures for the synthesis of **8** and **9**.

Table 1
Optimization of reaction conditions for **8**^a.

Entry	Solvent	32 (equiv.)	Et ₃ N (equiv.)	Temperature	Time (h)	Yield (%) ^b
1	acetic acid	1.5	no base	reflux	1	72 ^c
2	EtOH	1	no base	reflux	24	42 ^d
3	acetic acid	2	no base	reflux	40 min	85
4	EtOH (0.7 mL of acetic acid)	1	no base	reflux	16	47
5	DMF	2	1	110 °C	24	18
6	DMF	2	3	110 °C	24	45

^a The reaction was performed on 1.0 mmol scale of **32** in 2.5 mL of solvent at reflux.

^b Isolated yields.

^c Yield reported in literature = 72% [29].

^d Yield reported in literature = 100% [30].

was slightly more rapid (40 min) and, above all, more efficient (85% yield). Then, to understand whether the acid environment is essential for the outcome of the reaction, the experiment was repeated in EtOH but adding a catalytic amount of glacial acetic acid (entry 4). Results showed that the reaction led to the formation of **8** but less efficiently (47% yield) and much more slowly (16h) than that in glacial acetic acid. Then, we also repeated the reaction under basic conditions in the presence of different equiv. of Et₃N in DMF at 110 °C (entries 5 and 6). Both reactions did not finish after 24h (also waiting until 48h), furnishing **8** in 18% and 45% yield by using 1 equiv. and 3 equiv. of Et₃N, respectively. Thus, the best reaction conditions to synthesize compound **8** are treating **32** (2 equiv.)

and **33** (1 equiv.) in glacial acetic acid at reflux for 40 min (entry 3). Through this one-step procedure, compound **8** was regioselectively obtained in 85% yield.

The same authors reporting the synthesis of **8** in glacial acetic acid, also described the preparation of 2-amino-5-phenyl-[1,2,4] triazolo[1,5-*a*]pyrimidine (**9**) via cyclocondensation of **32** with 3-(dimethylamino)-1-phenyl-1-propanone hydrochloride (**34**) in glacial acetic acid at reflux, followed by heteroaromatization using NBS with a 29% overall yield (Scheme 1b) [29].

Thus, after preparation of compound **34** [32] via reaction of acetophenone with paraformaldehyde, dimethylamine hydrochloride and a catalytic amount of HCl in EtOH at reflux, we attempted

the synthesis of **9** by following the two-step procedure reported by Ribeiro et al. Interestingly, after the first reaction, we observed the formation of a mixture of 5-phenyl-4,7-dihydro-[1,2,4]triazolo[1,5-*a*]pyrimidin-2-amine and oxidized compound **9**. Prompted by this observation, we repeated the reaction in glacial acetic acid but in an open flask in order to promote the oxidation reaction, analogously to the synthesis of isomers **6** and **7** [25]. We observed an increase in the amount of **9**, although not reaching the complete oxidation of the 4,7-dihydro intermediate. Thus, we repeated the reaction under basic conditions by treating **32** (1 or 2 equiv.) and **34** (1 equiv.) in the presence of Et₃N (1 equiv.) in DMF at 110 °C in an open flask (entries 1 and 2, Table 2). We were pleased to find that these conditions regioselectively furnished only the already oxidized compound **9**, with the reaction performed by using 2 equiv. of **32** that was much more efficient (78% yield) and rapid (3h) than that performed by using 1 equiv. of **32** (56% yield after 5h). With these encouraging results, then, we studied the effect of the temperature (entry 3) or of the equiv. of Et₃N (entry 4), maintaining 2 equiv. of **32** and performing the reaction in DMF in an open flask. Results showed that the reaction performed at 120 °C is less efficient (55% yield) and rapid (6h) than that performed at 110 °C. On the other hand, the reaction performed with 2 equiv. of Et₃N is equally rapid (3h) and slightly less efficient (72% yield) than that performed with 1 equiv. of Et₃N. Finally, maintaining the best reaction conditions (2 equiv. of **32** and 1 equiv. of base at 110 °C in DMF in an open flask), we studied the effects of two different bases such as K₂CO₃ and Cs₂CO₃ (entries 5 and 6). Both reactions were equally rapid (5h), but the reaction performed with K₂CO₃ as base was more efficient (72% yield) than that performed with Cs₂CO₃ (50% yield). Thus, the optimum reaction conditions to synthesize compound **9** are treating **32** (2 equiv.) and **34** (1 equiv.) in DMF at 110 °C in an open flask for 3h in presence of Et₃N (1 equiv.) (entry 2). Through this one-step procedure, compound **9** was regioselectively obtained in 78% yield.

Then, we turned the attention to the synthesis of compounds 2-amino-6-phenyl-[1,2,4]triazolo[1,5-*a*]pyrimidine (**10**) and 2-amino-5-phenyl-[1,2,4]triazolo[1,5-*a*]pyrimidin-7-ol (**11**), whose syntheses are not known in literature.

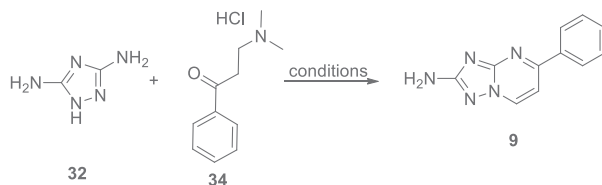
Regarding the preparation of compound **10**, we carried out the synthesis *via* reaction of **32** with *N*-[3-(dimethylamino)-2-phenylprop-2-en-1-ylidene]-*N*-methylmethanaminium perchlorate (**35**) (Table 3). Compound **35** [33] was synthesized as reported in literature *via* reaction of 2-phenylacetic acid with DMF and POCl₃ at 90 °C. We initially performed the reaction between **32** and **35** in glacial acetic acid at reflux (entry 1), but no significant reaction was

observed. Thus, we repeated the reaction under basic conditions treating **32** (2 equiv.) and **35** (1 equiv.) in the presence of Et₃N (1 equiv.) in *i*-PrOH at room temperature (rt) (entry 2). No starting material conversion was observed because of the insolubility of **32** in this solvent (also heating at 50 °C). Thus, we repeated the reaction in DMF, also studying the effect of different bases such as Et₃N (entry 3), NaH (entry 4) and K₂CO₃ (entry 5). We were pleased to find that all the reactions took place at rt rapidly (1h) and efficiently (92%, 54%, and 80% yield, respectively). Finally, the reaction was repeated in DMF in absence of a base (entry 6) furnishing **10** in 39% yield after 24h, thus showing that the basic environment significantly improves the reaction yield. Thus, the optimum reaction conditions to synthesize compound **10** are treating **32** (2 equiv.) and **35** (1 equiv.) in the presence of Et₃N (1 equiv.) in DMF at rt for 1h (entry 3). Through this one-step procedure, compound **10** was obtained in 92% yield.

Finally, we searched for a synthetic procedure for the preparation of 2-amino-5-phenyl-[1,2,4]triazolo[1,5-*a*]pyrimidin-7-ol (**11**) and carried out the synthesis *via* reaction of **32** with ethyl 3-oxo-3-phenylpropanoate (**36**) (Table 4). Also in this case, we initially performed the reaction in glacial acetic acid at reflux (entry 1), but still no significant reaction was observed after 24h. Thus, we repeated the reaction in DMF at 110 °C studying the effect of different bases such as NaH (entry 2), Et₃N (entry 3) and K₂CO₃ (entry 4). No significant reaction was observed in presence of Et₃N or NaH after 24h, while, after 12h, the reaction in presence of K₂CO₃ led to the regioselective formation of **11** although in 40% yield. To further explore the reaction conditions, the experiment was repeated in EtOH using EtONa as base (entry 5) and in *t*BuOH using *t*BuOK as base (entry 6) at reflux. Results showed that the reaction in EtOH was more rapid (12h) and efficient (66%) than that in *t*BuOH (24h, 54% yield). Based on this result, we then studied the effect of the equiv. of **32** (entry 7), of EtONa (entry 8), or both (entry 9) in EtOH at reflux. Both reactions performed with 2 equiv. of EtONa were less efficient furnishing **11** after 12h in 38 and 39% yield, while the reaction performed with 1 equiv. of **32** resulted the most efficient, yielding **11** after 12h in 79% yield. Thus, the best reaction conditions to synthesize compound **11** are treating **32** (1 equiv.) and **36** (1 equiv.) in EtOH in the presence of EtONa (1 equiv.) at reflux for 12h (entry 7). Through this one-step procedure, compound **11** was regioselectively obtained in 79% yield.

It is worthwhile to underline that all the compounds **8–11** were obtained pure from their relative procedures and did not require purification.

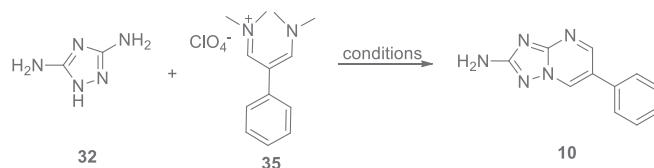
Table 2
Optimization of reaction conditions for **9**^a.



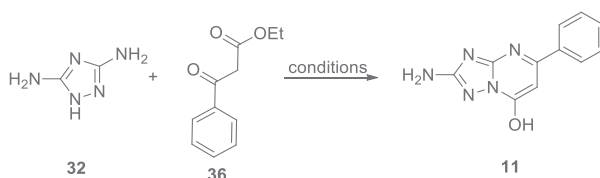
Entry	Solvent	32 (equiv.)	Base	Temperature	Time (h)	Yield (%) ^b
1	DMF	1	Et ₃ N, 1 equiv.	110 °C	5	56
2	DMF	2	Et ₃ N, 1 equiv.	110 °C	3	78
3	DMF	2	Et ₃ N, 1 equiv.	120 °C	6	55
4	DMF	2	Et ₃ N, 2 equiv.	110 °C	3	72
5	DMF	2	K ₂ CO ₃ , 1 equiv.	110 °C	5	72
6	DMF	2	Cs ₂ CO ₃ , 1 equiv.	110 °C	5	50

^a The reaction was performed on 1.0 mmol scale of **32** in 2.5 mL of solvent in an open flask.

^b Isolated yields.

Table 3
Optimization of reaction conditions for **10**^a.

Entry	Solvent	32 (equiv.)	Base (equiv.)	Temperature	Time (h)	Yield (%) ^b
1	acetic acid	1	no base	reflux	24	–
2	<i>i</i> -PrOH	2	Et ₃ N, 1 equiv.	50 °C	–	–
3	DMF	2	Et ₃ N, 1 equiv.	r.t.	1	92
4	DMF	2	NaH, 1 equiv.	r.t.	1	54
5	DMF	2	K ₂ CO ₃ , 1 equiv.	r.t.	1	80
6	DMF	2	no base	r.t.	24	39

^a The reaction was performed on 1.0 mmol scale of **32** in 2.5 mL of solvent at reflux.^b Isolated yields.**Table 4**
Optimization of reaction conditions for **11**^a.

Entry	Solvent	32 (equiv.)	Base	Temperature	Time (h)	Yield (%) ^b
1	acetic acid	1	no base	reflux	24	–
2	DMF	2	NaH, 1 equiv.	110 °C	24	–
3	DMF	2	Et ₃ N, 1 equiv.	110 °C	24	–
4	DMF	2	K ₂ CO ₃ , 1 equiv.	110 °C	12	40
5	EtOH	2	EtONa, 1 equiv.	reflux	12	66
6	<i>t</i> BuOH	2	<i>t</i> BuOK, 1 equiv.	reflux	24	54
7	EtOH	1	EtONa, 1 equiv.	reflux	12	79
8	EtOH	2	EtONa, 2 equiv.	reflux	12	39
9	EtOH	1	EtONa, 2 equiv.	reflux	12	38

^a The reaction was performed on 1.0 mmol scale of **32** in 2.5 mL of solvent at reflux.^b Isolated yields.

Regarding structural information, isomers **8** and **9** were previously described in literature [29], with the structure of compound **8** that was confirmed by crystallographic studies and was distinguished by that of compound **9** by NMR spectroscopy on the basis of the chemical shifts of the pyrimidine hydrogens (7.25 (H-6) and 8.53 (H-5) ppm for **8** and 7.72 (H-6) and 9.07 (H-7) ppm for **9**) and the coupling constant of pyrimidine hydrogens ($J = 4.8$ Hz for **8** and $J = 6.9$ Hz for **9**). On the other hand, compounds **10** and **11** herein reported were not described previously and their structures were fully characterized by spectral data of ¹H NMR, ¹³C NMR, and HRMS. In order to demonstrate the correct regioisomeric structure of compound **11** (C-5 -Ph, C-7 -OH), by comparing its ¹³C NMR spectrum to that of the analogue devoid of the amino group at the C(2) position [34], it is essential to consider the chemical shift of C(6) that is very similar for both **11** (98.4 ppm) and its close analogue (97.3 ppm); on the other hand, the chemical shift of C(6) of the 7-phenyl analogue devoid of the amino group at the C(2) position is 106.8 [35].

2.2. Reactivity of 3,5-diamino-1,2,4-triazole toward ambident electrophiles such as β -diketones, α,β -enones, β -enaminones, β -amino ketones and β -ketoesters

Based on the regioselectivity of the above reported reactions and those previously reported by us, we analyzed the reactivity of 3,5-diamino-1,2,4-triazole (**32**) towards different ambident electrophiles (Fig. 4). About the reactivity of **32**, we can assume that the presence of a second electron-donating amino group on the 1,2,4-triazole might be responsible for a higher nucleophilicity of the C(3) amino group than the N(2). Considering this hypothesized reactivity and based on the regioselectivity of previously reported reactions [25], it can be assumed that, when reacting with a β -diketone such **37**, the triazole C(3) amino group undergoes a direct addition at the C(3) carbonyl carbon and not at the C(1) carbonyl carbon of **37**, probably due to the steric hindrance of the phenyl group at the C(1). Analogously, when **32** reacts with α,β -enones such as **38** and **39**, independently from the hindrance of the

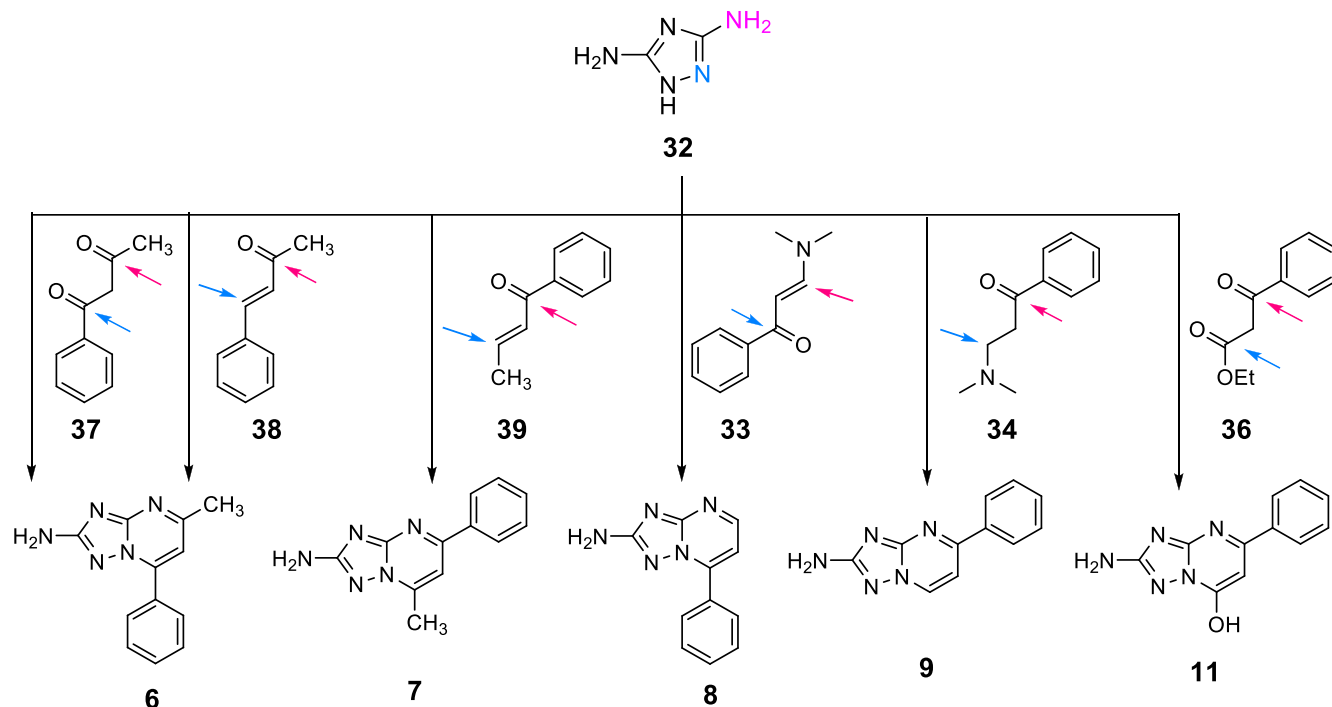


Fig. 4. Plausible reactivity of 3,5-diamino-1,2,4-triazole (**32**) toward ambident electrophiles such as β -diketone (**37**), α,β -enones (**38** and **39**), β -enaminone (**33**), β -amino ketone (**34**) and β -ketoester (**36**).

substituent on the carbonyl carbon, the triazole C(3) amino group seems to undergo the direct addition at the carbonyl carbon (C(2) of **38** and C(1) of **39**) [25], instead of a conjugated addition at the β -carbon (C(4) of **38** and C(3) of **39**).

Nevertheless, when **32** reacts with a β -enaminone such as **33**, the triazole C(3) amino group seems to prefer to undergo nucleophilic substitution at the β -carbon instead of the direct addition at the C(1) carbonyl carbon. Obviously, in the reaction of **32** with a β -amino ketone such as **34**, the triazole C(3) amino group conceivably undergoes a nucleophilic addition at the C(1) carbonyl carbon of **34**. Finally, it is worth to note that when reacting with a β -ketoester such as **36**, triazole C(3) amino group seems to prefer attacking the C(3) carbonyl carbon instead of the C(1) carbonyl carbon undergoing a direct addition rather than a nucleophilic substitution.

2.3. Synthesis of ethyl [1,2,4]triazolo[1,5-*a*]pyrimidine-2-carboxylates

To explore if the best reaction conditions determined for the synthesis of **8–11** could be applied for the preparation of ethyl [1,2,4]triazolo[1,5-*a*]pyrimidine-2-carboxylate analogues **14–17**, we repeated the reactions starting from ethyl 5-amino-1,2,4-triazole-3-carboxylate (**40**) (Scheme 2a). Results showed that the reaction of **40** with **33** in glacial acetic acid at reflux was equally rapid (40 min) as that starting from 3,5-diaminotriazole (**32**), furnishing compound **14** only slightly less efficiently (75% yield). On the contrary, the reactions of **40** with **34** and **35** in dry DMF at 110 °C and in the presence of Et₃N did not finish after 24h, furnishing, the first, a mixture of several products containing **15** only in traces and, the second, compound **16** in 23% yield. Finally, no starting material conversion was observed by reacting **40** with **36** in EtOH at reflux and using EtONa as a base.

To verify if acidic conditions could differently impact on reaction performance to obtain derivatives **15–17**, compound **40** was reacted with **34–36** in glacial acetic acid at reflux. Unfortunately, only

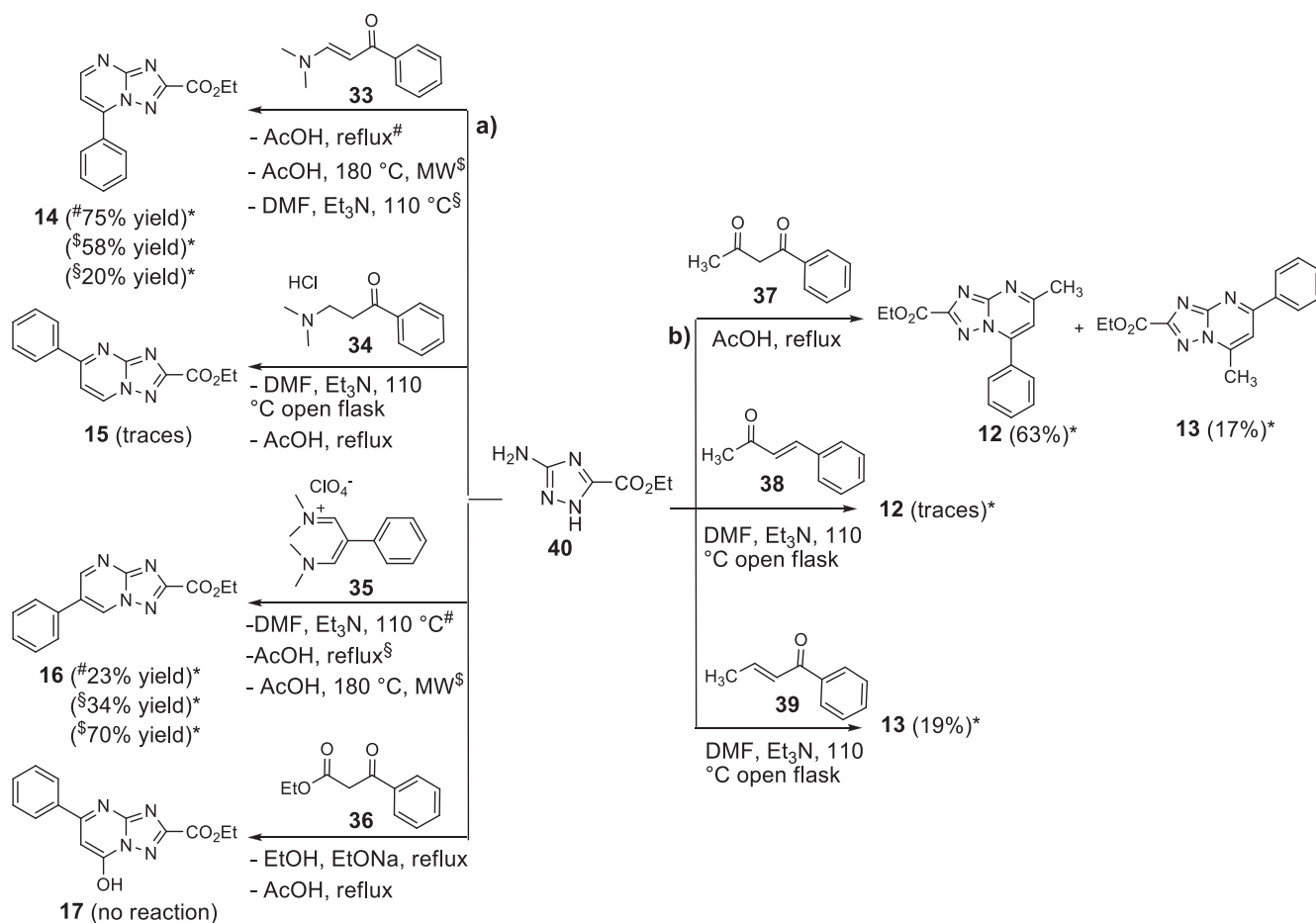
the reaction between **40** and **35** afforded the target compound **16**, although in 34% yield. However, the use of microwave irradiation improved the yield up to 70%, also reducing the time (40 min). Prompted from this observation, we also repeated the reaction between **40** and **33** in glacial acetic acid under microwave irradiation, but compound **14** was obtained in a lower yield (58%) than when using traditional heating. To complete the study, we also reacted **40** and **33** in DMF and Et₃N, observing that a basic environment strongly impaired the reaction yield (20%).

Of note, the scarce reactivity of **40** toward ambident electrophiles, due to the presence of an electron-withdrawing group at the C-2 position, was already observed by us during the preparation of ethyl 5-methyl-7-phenyl-[1,2,4]triazolo[1,5-*a*]pyrimidine-2-carboxylate (**12**) and 7-methyl-5-phenyl-[1,2,4]triazolo[1,5-*a*]pyrimidine-2-carboxylate (**13**) (Scheme 2b) [25]. In particular, the reaction of **40** with β -diketone **37** in glacial acetic acid at reflux was rapid (4h) and efficient (80% yield) but showed a dramatically decreased regioselectivity, furnishing **12** and **13** in the ratio of 3.7:1. On the other hand, the reaction of **40** with α,β -enones **38** and **39** (in DMF at 110 °C in the presence of Et₃N and in an open vessel) furnished after 24h isomers **12** and **13** in traces and 19% yield, respectively.

2.4. Design of antiviral compounds based on the [1,2,4]triazolo[1,5-*a*]pyrimidine structure

As a continuation of our previous efforts in identifying anti-IAV compounds able to inhibit RdRP PA-PB1 subunits interaction, in this work, we have synthesized additional analogues to better investigate the role of the substituents on the TZP core. Previously, starting from hit compound **1** [17], we synthesized a series of TZP analogues, mainly as hybrid compounds in which the TZP nucleus was joined with a thiophene-based core [19,24], while to date few biological data are available about the sole TZP nucleus [19,25].

Therefore, herein, about the TZP C-2 position, we studied the role of the 2-carbamoyl moiety on the (hetero)aromatic ring, which



Scheme 2. Synthesis of **14–17** via reaction of **40** with **33–36**, respectively, and known procedures for the synthesis of **12** and **13**. *Isolated yields.

previously emerged as important to achieve anti-PA-PB1 activity [19,24] in the 5-methyl-7-phenyl- and 7-methyl-5-phenyl-[1,2,4]triazolo[1,5-*a*]pyrimidine-2-carboxamide series. In particular, the carbamoyl moiety was replaced by a bioisosteric carboxylic acid in compounds **18** and **19**, also evaluating methyl ester intermediates **20** and **21**. Moreover, the amide linkage and the C-2 carboxylic group of compounds **18** and **19** were constrained into a benzo[*d*] [1,3]oxazin-4-one ring, giving derivatives **22** and **23**.

Focusing the attention on the C-5, C-6, and C-7 positions of the TZP core, the presence of a sole phenyl ring in each of these positions was explored by using scaffolds **8–11**, which were functionalized with an unsubstituted benzoyl moiety at the C-2 position, analogously to hit compound **2**. Compounds **24–26** were thus prepared along with compound **27**, where the 5-phenyl ring was coupled with a hydroxyl group at the C-7 position.

Unfortunately, synthetic issues impaired the functionalization of scaffolds **8–11** with a 2-carbamoylphenyl moiety, thus, we decided to use an inverse amide to introduce this moiety.

As reported above, we were able to synthesize only ethyl [1,2,4]triazolo[1,5-*a*]pyrimidine-2-carboxylate **14** and **16**, which were functionalized to give compounds **28** and **29**, respectively. Additionally, analogues **30** and **31** were prepared, selecting as C-2 substituent the cycloheptathiophene-3-carboxamide moiety characterizing compounds **4** and **5**.

2.5. Synthesis of the target compounds 18–31

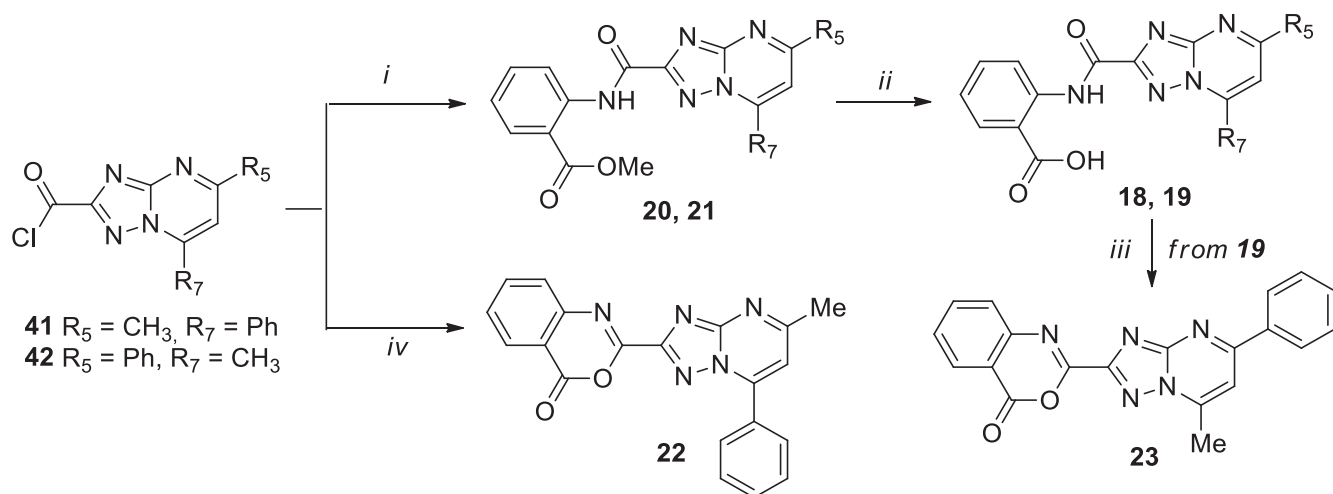
Compounds **18** and **19** were synthesized, as reported in Scheme

3, by coupling reaction of 5-methyl-7-phenyl-[1,2,4]triazolo[1,5-*a*]pyrimidine-2-carbonyl chloride **41** [19] and 7-methyl-5-phenyl-[1,2,4]triazolo[1,5-*a*]pyrimidine-2-carbonyl chloride **42** [19] with methyl 2-aminobenzoate in CH₂Cl₂ in presence of DIPEA at rt, to give methyl esters **20** and **21**. The successive hydrolysis of compounds **20** and **21** in the presence of LiOH in H₂O/THF mixture at 50 °C furnished acid derivatives **18** and **19**, of which **19** was in turn cyclized in acetic anhydride at 100 °C furnishing benzooxazinone derivative **23**. Actually, the synthesis of compounds **22** and **23** was initially attempted via reaction of **41** [19] and **42** [19] with 2-aminobenzoic acid in CH₂Cl₂ in presence of DIPEA at rt, but only compound **22** was successfully obtained, while the reaction starting from **42** furnished only acid intermediate **19**.

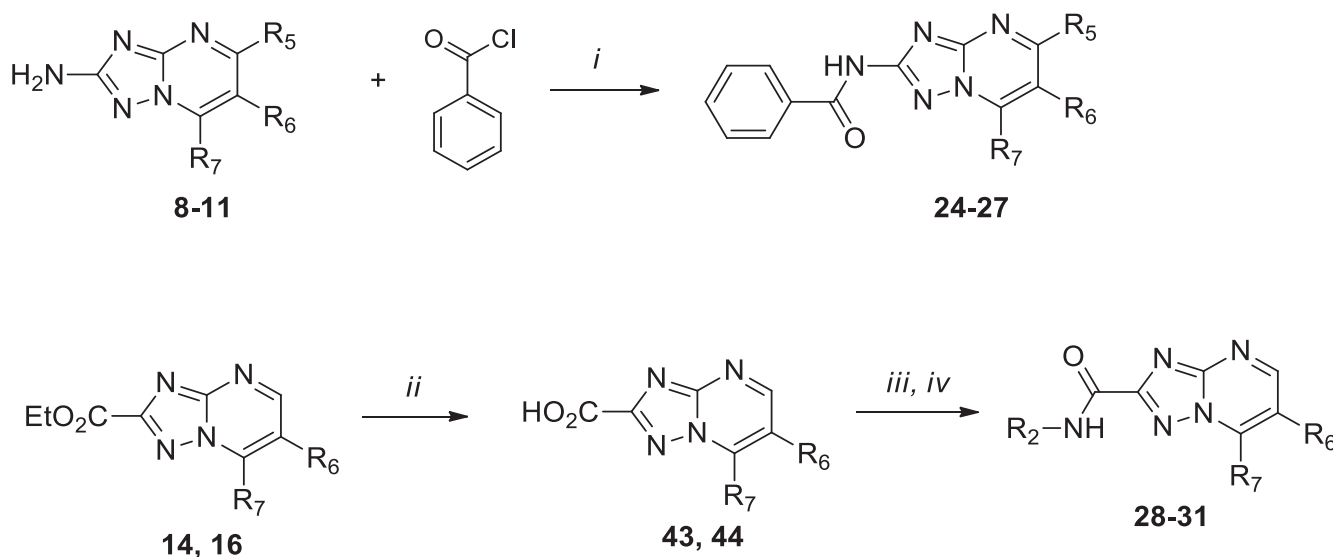
Compounds **24–27** were synthesized via reaction of **8–11** with benzoyl chloride in pyridine at 80 °C, as reported in Scheme 4. Finally, target compounds **28–31** were synthesized starting from compounds **14** and **16**, which were hydrolysed under basic conditions, to give intermediates **43** and **44**, chlorinated, and reacted with 2-aminobenzamide or 2-amino-5,6,7,8-tetrahydro-4*H*-cyclohepta[*b*]thiophene-3-carboxamide in CH₂Cl₂ in the presence of DIPEA (Scheme 4).

2.6. Evaluation of antiviral activity

Compounds **18–31** were evaluated for the ability to inhibit the physical interaction between IAV PA and PB1 subunits by ELISA including the Tat-PB1_{1–15} peptide as a positive control of inhibition. In parallel, for all the synthesized compounds, the antiviral activity



Scheme 3. Synthesis of target compounds **18–23**. Reagents: i) methyl 2-aminobenzoate, DIPEA, CH_2Cl_2 , rt; ii) LiOH , $\text{H}_2\text{O}/\text{THF}$ (1:1), 50°C ; iii) Ac_2O , 100°C ; iv) 2-aminobenzoic acid, DIPEA, CH_2Cl_2 , rt.



Scheme 4. Synthesis of target compounds **24–31**. Reagents: i) pyridine 80°C ; ii) NaOH , MeOH , reflux; iii) oxalyl chloride, CH_2Cl_2 , DMF , rt; iv) 2-aminobenzamide or 2-amino-5,6,7,8-tetrahydro-4*H*-cyclohepta[*b*]thiophene-3-carboxamide, DIPEA, CH_2Cl_2 , rt.

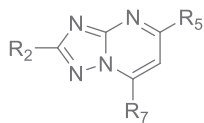
was tested by plaque reduction assays (PRA) in Madin-Darby canine kidney (MDCK) cells infected with a reference IAV, the A/PR/8/34 strain. Ribavirin (RBV), a known broad-spectrum inhibitor of RNA virus polymerases, was also included. To exclude that the observed antiviral activities could be due to toxic effects on the target cells, the compounds were also tested by MTT assays in MDCK cells.

As shown in Table 5, compounds **24–27** were devoid of both the abilities to dissociate PA-PB1 interaction and inhibit viral replication.

On the other hand, when the TZP scaffolds having a C-6 or C-7 phenyl ring and the inverse amide were functionalized with a 2-carbamoylphenyl moiety at the C-2 position (compounds **28** and **29**), efficient inhibition of PA-PB1 interaction was achieved ($\text{IC}_{50} = 21 \mu\text{M}$). Of note, the same anti-PA-PB1 activity ($\text{IC}_{50} = 22 \mu\text{M}$) was shown by 6-phenyl TZP compound **31** functionalized at the C-2 position with a cycloheptathiophene-3-carboxamide moiety. Nevertheless, all compounds **28–31** were devoid of antiviral activity.

Finally, efficient ability to disrupt PA-PB1 heterodimerization was also shown by four of the six compounds based on scaffolds **6** and **7**, with IC_{50} values ranging from 19.5 to $32 \mu\text{M}$. Also in this case, the compounds did not show antiviral activity, with the exception of compound **22** that besides displaying the best anti-PA-PB1 activity ($\text{IC}_{50} = 19.5 \mu\text{M}$, Figure S1), also showed a good anti-IAV activity ($\text{EC}_{50} = 16 \mu\text{M}$, Figure S2 and S3), thus resulting among the most active TZP derivative reported to date by us. Of note, all compounds **18–31** were non-toxic up to $250 \mu\text{M}$ concentration (Figure S4, for compound **22**), with the exception of compound **31** that showed mild cytotoxicity ($\text{CC}_{50} = 100 \mu\text{M}$). Based on these data, some SAR insights can be drawn: i) the 7-methyl-5-phenyl- and 5-methyl-7-phenyl-TZP series were better than compounds having only a phenyl ring at the C-5, C-6 or C-7 positions of the TZP core; ii) among the 7-methyl-5-phenyl-TZP and 5-methyl-7-phenyl-TZP series, the activity of the compounds is strictly dependent on the substituent at the C-2 position of the TZP nucleus; iii) focusing on the C-2 substituent, the 2-carbamoylphenyl ring was the best within the 7-methyl-5-phenyl-TZP series, while

Table 5
Structure and Anti-IAV Activity of [1,2,4]triazolo[1,5-*a*]pyrimidine derivatives.



Compd	R ₂	R ₅	R ₇	ELISA PA-PB1 Interaction Assay IC ₅₀ , μM ^a	PRA in MDCK cells EC ₅₀ , μM ^b	Cytotoxicity in MDCK cells CC ₅₀ , μM ^c
18		CH ₃	C ₆ H ₅	116 ± 43	>100	>250
19	"	C ₆ H ₅	CH ₃	32 ± 14	>100	>250
20		CH ₃	C ₆ H ₅	26.5 ± 2.1	>80	>250
21	"	C ₆ H ₅	CH ₃	22.3 ± 6.4	>100	>250
22		CH ₃	C ₆ H ₅	19.5 ± 4.9	16 ± 5.7	>250
23	"	C ₆ H ₅	CH ₃	123 ± 45	>100	>200

Compd	R ₅	R ₆	R ₇	ELISA PA-PB1 Interaction Assay IC ₅₀ , μM ^a	PRA in MDCK cells EC ₅₀ , μM ^b	Cytotoxicity (MTT Assay) in MDCK cells CC ₅₀ , μM ^c
24	H	H	C ₆ H ₅	>200	>100	>250
25	C ₆ H ₅	H	H	165	>100	>250
26	H	C ₆ H ₅	H	>200	>100	>250
27	C ₆ H ₅	H	OH	113 ± 46	>100	>250

Compd	R ₂	R ₆	R ₇	ELISA PA-PB1 Interaction Assay IC ₅₀ , μM ^a	PRA in MDCK cells EC ₅₀ , μM ^b	Cytotoxicity (MTT Assay) in MDCK cells CC ₅₀ , μM ^c
28		H	C ₆ H ₅	21 ± 4.2	>100	>250
29	"	C ₆ H ₅	H	21 ± 8	>100	>250
30		H	C ₆ H ₅	>200	>60	>200
31	"	C ₆ H ₅	H	22 ± 3	>100	100 ± 9
Tat-PB1₁₋₁₅ peptide				35 ± 4	41 ± 5	>100
RBV					10 ± 2	>250

^a Activity of the compounds in ELISA PA-PB1 interaction assays. The IC₅₀ value represents the compound concentration that reduces by 50% the interaction between PA and PB1.

^b Activity of the compounds in plaque reduction assays with the IAV A/PR/8/34 strain. The EC₅₀ value represents the compound concentration that inhibits 50% of plaque formation.

^c Cytotoxicity of the compounds in MTT assays. The CC₅₀ value represents the compound concentration that causes a decrease of cell viability by 50%. All the reported values represent the means ± SD of data derived from at least three independent experiments in duplicate.

within the 5-methyl-7-phenyl-TZP series, the benzooxazinone imparted the best activity thus emerging as a new moiety to be further investigated; iv) regarding the amide linkage, an inverse amide permitted a wider functionalization of the C-2 TZP, which instead was not permitted starting from a 2-amino-TZP, thus it was not possible to determine the best linkage by comparing strict analogues.

Then, we investigated the ability of compound **22** to interfere with the catalytic activity of IAV RdRP in a cellular context by a minireplicon assay in HEK 293T cells. Compound **22** exhibited an EC₅₀ of 21 ± 3 μM (Figure S5) at non-toxic concentration (CC₅₀ > 150 μM), thus confirming its ability to inhibit RdRP functions by interfering with PA-PB1 heterodimerization; RBV was used as reference control (EC₅₀ = 16 ± 2 μM, CC₅₀ > 250 μM).

In the course of this work, the global population has been affected by the COVID-19 pandemic, caused by the severe acute respiratory syndrome coronavirus 2 (SARS-CoV-2). Developing new treatments is typically a lengthy process, while repurposing existing compounds is a potential accelerated way to find an urgently needed treatment. Having in house a library of drug-like compounds, of which many were developed as antiviral agents, a set of 31 TZP-based compounds, including seven of the derivatives herein reported (compounds **19**, **21–23**, **25**, **26** and **31**), was also evaluated for their activity against SARS-CoV-2. In a first round of screening, all compounds were evaluated in duplicate at 4 concentrations (100, 20, 4, and 0.8 μM) as potential inhibitors of SARS-CoV-2 replication in a cell context. Initially, only antiviral activity, but no cytotoxicity was measured. From this initial screening, five TZPs (compounds **45–49**) emerged as weak inhibitors of SARS-CoV-2, with extrapolated EC₅₀ values in the range of 30–65 μM (Table 6). One analogue from this series (compound **49**) was subjected to a full dose-response analysis (Figure S6) with simultaneous determination of the cytotoxicity in Vero E6 cells. This compound showed anti-SARS-CoV-2 activity with an EC₅₀ value of 34.47 μM and lacked cytotoxicity at the highest tested concentration (*i.e.* 100 μM). GS-441524, the parent nucleoside analogue of remdesivir [36], was included as positive control and reference compound. This compound was endowed with an EC₅₀ and CC₅₀ values of 0.89 μM and 72.38 μM, respectively.

Based on the emerged SAR insights, the compounds showing anti-SARS-CoV-2 activity belong to the series of 5-phenyl-7-methyl-TZPs, while compounds having a phenyl ring at the C-6 or C-7 position resulted inactive. Regarding the C-2 position, an unsubstituted phenyl ring (compound **45**) imparted the same activity of a *p*-NH₂ phenyl ring (compound **48**), which instead slightly decreased with a *p*-OPr phenyl moiety (compound **46**) and completely fell with *p*-OMe, *p*-NO₂ and 3,4-di-OH phenyl moieties (compounds **50–52**, respectively). On the other hand, the activity slightly increased with a *o*-F phenyl moiety at the C-2 position (compound **47**) and this activity was maintained also inverting the amide linkage, as shown by compound **49**.

Finally, trying to highlight common SAR insights for IAV and SARS-CoV-2, we herein evaluated the anti-IAV activity of compounds **47** [37], **48** [37], **49**, **51** [37] and **52** [37], and their activity was reported in Table 6, along with those of compounds **45** [19], **46** [19] and **50** [19]. No common SAR insights have been found, although derivatives **45** and **49**, belonging to 5-phenyl-7-methyl-TZP class, showed both antiviral activities. Of note, compound **49** also exhibited good anti-PA-PB1 activity with an IC₅₀ value of 17.5 μM.

3. Conclusions

In this work, four efficient one-step procedures for the synthesis of 5-phenyl-, 6-phenyl- and 7-phenyl-2-amino-[1,2,4]triazolo[1,5-

a]pyrimidines, and 2-amino-5-phenyl-[1,2,4]triazolo[1,5-*a*]pyrimidin-7-ol have been developed, under mild conditions, with high yields (ranging from 85% to 92%), and regioselectivity for compounds **8**, **9** and **11**. Of note, the one-step procedure used for the synthesis of **9** resulted much more efficient (78%) than the two-steps procedure reported in literature (29%), but, above all, avoided the oxidation reaction by NBS or Br₂, which being highly reactive limit the choice of substituents on the TZP. The synthesis of the four analogues having the ethyl carboxylate moiety at the C-2 position of the TZP structure was also attempted, leading to synthesize 7-phenyl derivative **14** and 6-phenyl derivative **16** in good yields (75% and 70%, respectively).

Subsequently, the synthesized scaffolds have been used for the synthesis of a set of TZP derivatives as anti-IAV compounds acting by disrupting viral RdRP PA-PB1 subunits interaction. From the biological evaluation, compound **22** inhibited PA-PB1 interaction with an IC₅₀ of 19.5 μM, RdRP functions with an EC₅₀ of 21 μM and viral replication with an EC₅₀ of 16 μM, and not showing cytotoxicity up to 250 μM.

Although good results have been achieved in this work, further efforts are required to enhance the antiviral potency and better characterize PA-PB1 inhibitory properties through: i) co-crystallization studies and mutagenesis experiments in order to guide the hit-optimization; ii) co-administration with approved agents; and iii) the evaluation of the anti-IAV activity in an animal model.

Interestingly, the TZP derivative **49** also showed anti-SARS-CoV-2 activity with an EC₅₀ value of 34.47 μM and lacking cytotoxicity on Vero E6 cells. This activity could be due to a mechanism of action involving a PPI inhibition, as suggested from its ability to interfere with PA-PB1 heterodimerization (IC₅₀ = 17.5 μM). Further studies will be devoted to investigating this hypothesis.

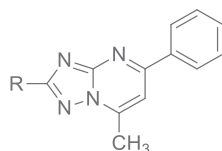
4. Experimental section

4.1. Chemistry

Commercially available starting materials, reagents, and solvents were used as supplied. Compounds 3-(dimethylamino)-1-phenyl-2-propen-1-one (**33**) [31], 3-(dimethylamino)-1-phenyl-1-propanone hydrochloride (**34**) [32], and *N*-[3-(dimethylamino)-2-phenylprop-2-en-1-ylidene]-*N*-methylmethanaminium (**35**) [33] were synthesized as reported in literature. Compound 3-oxo-3-phenylpropanoate (**36**) was purchased from Alfa Aesar. Compound ethyl 5-amino-1,2,4-triazole-3-carboxylate (**40**) [38] was synthesized as reported in literature. Compounds 5-methyl-7-phenyl-[1,2,4]triazolo[1,5-*a*]pyrimidine-2-carbonyl chloride (**41**) [19] and 7-methyl-5-phenyl-[1,2,4]triazolo[1,5-*a*]pyrimidine-2-carbonyl chloride (**42**) [19] were synthesized as previously reported by us. Synthesis of compound **49**, which entailed the reaction of **42** [19] with *o*-fluoroaniline in pyridine at 80 °C, was not reported previously and herein included.

All reactions were routinely monitored by TLC on silica gel 60F254 (Merck) and visualized by using UV or iodine. Flash column chromatography was performed on Merck silica gel 60 (mesh 230–400). After extraction, organic solutions were dried over anhydrous Na₂SO₄, filtered, and concentrated with a Büchi rotary evaporator at reduced pressure. Yields are of purified product and were not optimized. HRMS spectra were registered on Agilent Technologies 6540 UHD Accurate Mass Q-TOF LC/MS, HPLC 1290 Infinity. Purities of compounds **18–31** were determined by LC/MS using an Agilent 1290 Infinity System machine equipped with DAD detector from 190 to 640 nm. The purity was revealed at 254 nm using a Phenomenex AERIS Widepore C4, 4.6 mm, 100 mm (6.6 lm) with flow rate: 0.85 ml/min; acquisition time: 10 min; gradient:

Table 6
Structure and anti-SARS-CoV-2 activity of [1,2,4]triazolo[1,5-*a*]pyrimidine derivatives.



Compd	R	Anti-SARS-CoV-2 activity EC ₅₀ (μM) ^a	VeroE6 cells CC ₅₀ (μM) ^b	PRA in MDCK cells EC ₅₀ , μM ^c	Cytotoxicity (MTT Assay) in MDCK cells CC ₅₀ , μM ^c
45		44.36 ± 10.35	ND ^d	25	>250
46		65.35 ± 3.52	ND	>100	247
47		30.61 ± 10.69	ND	>100	>250
48		43.96 ± 7.80	ND	>100	>250
49^e		34.47 ± 2.99	>100	83.8 ± 19.8	>250
50		>100	ND	>100	>250
51		>100	ND	>100	>250
52		>100	ND	>100	112
GS-441524		0.89 ± 0.62	72.38 ± 11.57		

^a EC₅₀ = concentration of compound that gives 50% rescue of the virus-reduced eGFP signals as compared to the untreated virus-infected control cells.

^b CC₅₀ = 50% cytotoxic concentration, as determined by measuring the cell viability with the colorimetric formazan-based MTS assay. The values represent the means ± SD of data derived from duplicate experiments.

^c For the definition of EC₅₀ and CC₅₀, see Table 5.

^d ND = not determined.

^e IC₅₀ = 17.5 ± 3.5 μM (ELISA PA-PB1 Interaction Assay).

acetonitrile in water containing 0.1% of formic acid (0100% in 10 min); oven temperature, 30°C. Peak retention time is given in minutes. ¹H NMR and ¹³C NMR spectra were recorded on Bruker Avance DRX-400MHz using residual solvents such as dimethylsulfoxide ($\delta = 2.48$) or chloroform ($\delta = 7.26$) as an internal standard. Chemical shifts were recorded in ppm (δ) and the spectral data are consistent with the assigned structures. The spin multiplicities are indicated by the: symbols s (singlet), d (doublet), t (triplet), q (quartet), m (multiplet), and bs (broad singlet).

4.1.1. 2-Amino-7-phenyl-[1,2,4]triazolo[1,5-*a*]pyrimidine (**8**) [29]

A mixture of **32** (0.1 g, 1 mmol) and **33** [31] (0.09 g, 0.5 mmol) in glacial acetic acid (2.5 mL) was refluxed for 40 min. After cooling, the reaction mixture was evaporated to dryness, obtaining a solid that was treated with ice/water and filtered to give **8** (0.18 g, 85%) as a white solid. ¹H NMR (400 MHz, DMSO-*d*₆) δ : 6.42 (s, 2H, NH₂), 7.21 (d, *J* = 4.9 Hz, 1H, H-6), 7.52–7.58 (m, 3H, Ar-H), 8.10–8.14 (m, 2H, Ar-H), 8.50 (d, *J* = 4.9 Hz, 1H, H-7); ¹³C NMR (101 MHz, DMSO-*d*₆) δ : 107.5, 128.8, 129.6, 130.6, 131.5, 144.9, 151.9, 156.4, 167.7. HRMS: *m/z* calcd for C₁₁H₉N₅ 212.0937 (M + H⁺), found 212.0936 (M + H⁺).

4.1.2. 2-Amino-5-phenyl-[1,2,4]triazolo[1,5-*a*]pyrimidine (**9**) [29]

To a mixture of **32** (0.1 g, 1 mmol) and **34** [32] (0.1 g, 0.5 mmol) in DMF (2.5 mL), Et₃N (0.07 mL, 0.5 mmol) was added and the reaction mixture was heated at 110 °C for 3 h maintaining open the flask. After cooling, the reaction mixture was poured into ice/water obtaining a precipitate that was filtered. The filtrate was extracted with EtOAc and the organic layers were evaporated to dryness, giving a solid that was combined with the precipitate previously filtered, to give **9** (0.083 g, 78%) a yellow solid. ¹H NMR (400 MHz, DMSO-*d*₆) δ : 6.36 (s, 2H, NH₂), 7.49–7.53 (m, 3H, Ar-H), 7.57 (d, *J* = 6.9 Hz, 1H, H6), 8.13–8.15 (m, 2H, Ar-H), 8.95 (d, *J* = 6.9 Hz, 1H, H7); ¹³C NMR (101 MHz, DMSO-*d*₆) δ : 105.0, 127.4, 129.3, 130.9, 135.1, 136.8, 155.3, 158.0, 168.3. HRMS: *m/z* calcd for C₁₁H₉N₅ 212.0937 (M + H⁺), found 212.0935 (M + H⁺).

4.1.3. 2-Amino-6-phenyl-[1,2,4]triazolo[1,5-*a*]pyrimidine (**10**)

To a mixture of **32** (0.1 g, 1 mmol) and **35** [33] (0.15 g, 0.5 mmol) in dry DMF (2.5 mL), dry Et₃N (0.07 mL, 0.5 mmol) was added under nitrogen atmosphere. The reaction mixture was maintained at rt for 1h, and then evaporated to dryness obtaining a solid that was

treated with ice/water and filtered to give **10** (0.098 g, 92%) as a white solid. ^1H NMR (400 MHz, DMSO- d_6) δ : 6.45 (s, 2H, NH₂), 7.38 (t, J = 7.4 Hz, 1H, Ar-H), 7.46 (t, J = 7.4 Hz, 2H, Ar-H), 7.75 (d, J = 7.4 Hz, 2H, Ar-H), 8.80 (d, J = 2.0 Hz, 1H, H7), 9.28 (d, J = 2.0 Hz, 1H, H5); ^{13}C NMR (101 MHz, DMSO- d_6) δ : 121.6, 127.0, 128.4, 129.5, 132.1, 133.9, 151.1, 154.6, 168.2. HRMS: m/z calcd for C₁₁H₉N₅ 212.0937 (M + H⁺), found 212.0935 (M + H⁺).

4.1.4. 2-Amino-5-phenyl-[1,2,4]triazolo[1,5-*a*]pyrimidin-7-ol (**11**)

To a mixture of **32** (0.1 g, 1 mmol) and **36** (0.17 mL, 1 mmol) in dry EtOH (2.5 mL), freshly prepared NaOEt (0.068 g, 1 mmol) was added under a nitrogen atmosphere and the reaction mixture was refluxed for 12h. After cooling, it was poured into ice/water and acidified until pH 6 with a 2 N HCl, obtaining a precipitate that was filtered to give **11** (0.18 g, 79%) as white solid. ^1H NMR (400 MHz, DMSO- d_6) δ : 6.16 (s, 1H, H-6), 7.45–7.48 (m, 3H, Ar-H), 7.81–7.84 (m, 2H, Ar-H); ^{13}C NMR (101 MHz, DMSO- d_6) δ : 98.4, 127.4, 129.1, 130.7, 134.7, 150.6, 153.0, 155.8, 159.9. HRMS: m/z calcd for C₁₁H₉N₅O 228.0886 (M + H⁺), found 228.0882 (M + H⁺).

4.1.5. Ethyl 7-phenyl-[1,2,4]triazolo[1,5-*a*]pyrimidine-2-carboxylate (**14**)

Method 1: the title compound was prepared by using the same procedure as used for the synthesis of **8** starting from **40** [38] (40 min), in 75% yield as white solid.

Method 2: the title compound was prepared by using the same conditions as used for the synthesis of **8** starting from **40** [38], but performing the reaction under microwave irradiation; after 40 min at 180 °C, the reaction was poured into ice/water and a precipitate was obtained and filtered to give **14** in 58% yield as white solid.

^1H NMR (400 MHz, DMSO- d_6) δ : 1.35 (t, J = 7.0 Hz, CH₂CH₃), 4.43 (q, J = 7.0 Hz, CH₂CH₃), 7.64–7.67 (m, 3H, Ar-H), 7.71 (d, J = 4.6 Hz, 1H, H-6), 8.13–8.15 (m, 2H, Ar-H), 9.05 (d, J = 4.3 Hz, 1H, H-5); ^{13}C NMR (101 MHz, DMSO- d_6) δ : 14.0, 61.8, 111.3, 128.7, 129.3, 129.5, 131.8, 147.9, 155.9, 156.1, 156.6, 159.9. HRMS: m/z calcd for C₁₄H₁₂N₄O₂ 269.1039 (M + H⁺), found 269.1039 (M + H⁺).

4.1.6. Ethyl 6-phenyl-[1,2,4]triazolo[1,5-*a*]pyrimidine-2-carboxylate (**16**)

Method 1: The title compound was prepared by using the same procedure as used for the synthesis of **8** starting from **40** [38] and replacing **33** with **35** (24 h), in 34% yield as white solid.

Method 2: the title compound was prepared by using the same conditions as used for the synthesis of **8** starting from **40** [38] and replacing **33** with **35**, but performing the reaction under microwave irradiation; after 40 min at 180 °C, the reaction was poured into ice/water and a precipitate was obtained and filtered to give **16** in 70% yield as white solid.

^1H NMR (400 MHz, CDCl₃) δ : 1.51 (t, J = 7.0 Hz, 3H, CH₂CH₃), 4.59 (q, J = 7.0 Hz, 2H, CH₂CH₃), 7.54–7.62 (m, 5H, Ar-H), 9.02 (d, J = 2.4, 1H, H7), 9.20 (d, J = 2.4, 1H, H5); ^{13}C NMR (101 MHz, DMSO- d_6) δ : 14.0, 61.8, 125.4, 127.4, 129.1, 129.3, 132.4, 134.5, 154.0, 156.6, 156.7, 159.7. HRMS: m/z calcd for C₁₄H₁₂N₄O₂ 269.1039 (M + H⁺), found 269.1040 (M + H⁺).

4.1.7. General procedure for the synthesis of compounds **20–22** and **28–31** by amidation

(Method A). To a solution of the appropriate [1,2,4]triazolo[1,5-*a*]pyrimidine-2-carboxylic acid (2 mmol) in dry CH₂Cl₂ (20 mL), oxalyl chloride (12 mmol) was added and after 30 min dry DMF (2 drops) was added. After 2 h stirring at rt, the reaction mixture was evaporated to dryness to give a residue that was dissolved in dry CH₂Cl₂ and added of the appropriate aniline (2 mmol) and DIPEA (2 mmol). The reaction was maintained at rt for 2 h and then evaporated to dryness to give a residue that was treated with ice/

water to give a solid that was filtered and purified as described below.

4.1.8. Methyl 2-(5-methyl-7-phenyl-[1,2,4]triazolo[1,5-*a*]pyrimidine-2-carboxamido)benzoate (**20**)

The title compound was prepared starting from **41** [19] and methyl 2-aminobenzoate by Method A and purified by flash chromatography eluting with CHCl₃/MeOH (99:1) in 43% yield. ^1H NMR (400 MHz, CDCl₃): δ 2.86 (s, 3H, CH₃), 4.06 (s, 3H, OCH₃), 7.22 (t, J = 7.5 Hz, 1H, Ar-H), 7.31 (s, 1H, H6), 7.65–7.69 (m, 4H, Ar-H), 8.16 (d, J = 8.0 Hz, 1H, Ar-H), 8.25–8.27 (m, 2H, Ar-H), 9.04 (d, J = 8.5 Hz, 1H, Ar-H), 12.94 (s, 1H, NH); ^{13}C NMR (101 MHz, CDCl₃): δ 25.5, 52.6, 111.1, 116.2, 120.9, 123.4, 129.1, 129.3, 129.7, 131.1, 132.1, 134.7, 140.8, 147.8, 156.5, 157.9, 159.9, 166.5, 168.2. HRMS: m/z calcd for C₂₁H₁₇N₅O₃ 388.1429 (M + H⁺), found 388.1412 (M + H⁺). HPLC, ret. time: 7.26 min, peak area: 98.89%.

4.1.9. Methyl 2-(7-methyl-5-phenyl-[1,2,4]triazolo[1,5-*a*]pyrimidine-2-carboxamido)benzoate (**21**)

The title compound was prepared starting from **42** [19] and methyl 2-aminobenzoate by Method A and purified by flash chromatography eluting with CHCl₃/MeOH (99:1) in 40% yield. ^1H NMR (400 MHz, CDCl₃): δ 3.02 (s, 3H, CH₃), 4.04 (s, 3H, OCH₃), 7.19 (t, J = 7.6 Hz, 1H, Ar-H), 7.52 (s, 1H, H6), 7.54–7.57 (m, 3H, Ar-H), 7.64 (t, J = 7.2 Hz, 1H, Ar-H), 8.13 (dd, J = 1.6 and 8.0 Hz, 1H, Ar-H), 8.23–8.25 (m, 2H, Ar-H), 9.00 (d, J = 8.4 Hz, 1H, Ar-H), 12.88 (s, 1H, NH); ^{13}C NMR (101 MHz, CDCl₃): δ 17.8, 52.7, 108.4, 116.2, 121.1, 123.5, 128.0, 129.2, 131.2, 131.7, 134.7, 136.1, 140.7, 148.4, 155.7, 158.0, 160.2, 162.5, 168.2. HRMS: m/z calcd for C₂₁H₁₇N₅O₃ 388.1427 (M + H⁺), found 388.1411 (M + H⁺). HPLC, ret. time: 9.60 min, peak area: 99.68%.

4.1.10. 2-(5-Methyl-7-phenyl-[1,2,4]triazolo[1,5-*a*]pyrimidine-2-carboxamido)benzoic acid (**18**)

A suspension of **20** (0.05 g, 0.13 mmol) and LiOH (0.02 g, 0.51 mmol) in a mixture H₂O/THF (1:1, 5 mL) was maintained at 50 °C for 3h. After cooling the reaction mixture was acidified (pH 5–6) with 2 N HCl obtaining a precipitate that was filtered and crystallized by EtOH/DMF to give **18** (0.035 g, 73% yield). ^1H NMR (400 MHz, DMSO- d_6): δ 2.74 (s, 3H, CH₃), 7.26 (t, J = 7.6 Hz, 1H, Ar-H), 7.68–7.72 (m, 5H, Ar-H and H6), 8.09 (d, J = 7.9 Hz, 1H, Ar-H), 8.24–8.26 (m, 2H, Ar-H), 8.81 (d, J = 8.4 Hz, 1H, Ar-H), 12.85 (s, 1H, NH), 13.75 (bs, 1H, COOH); ^{13}C NMR (101 MHz, DMSO- d_6): δ 24.8, 111.8, 116.8, 119.9, 123.5, 128.8, 129.3, 129.6, 131.4, 131.8, 134.3, 140.1, 146.6, 155.6, 157.4, 158.3, 166.8, 169.1. HRMS: m/z calcd for C₂₀H₁₅N₅O₃ 374.1260 (M + H⁺), found 374.1250 (M + H⁺). HPLC, ret. time: 3.97 min, peak area: 99.16%.

4.1.11. 2-(7-Methyl-5-phenyl-[1,2,4]triazolo[1,5-*a*]pyrimidine-2-carboxamido)benzoic acid (**19**)

The title compound was obtained starting from **21** by using the same procedure as used for the synthesis of **18** in 43% yield after crystallization by EtOH/DMF. ^1H NMR (400 MHz, DMSO- d_6): δ 2.91 (s, 3H, CH₃), 7.27 (t, J = 7.6 Hz, 1H, Ar-H), 7.62–7.63 (m, 3H, Ar-H), 7.71 (t, J = 7.9 Hz, 1H, Ar-H), 8.09 (d, J = 7.8 Hz, 1H, Ar-H), 8.14 (s, 1H, H6), 8.31–8.33 (m, 2H, Ar-H), 8.84 (d, J = 8.3 Hz, 1H, Ar-H), 12.90 (s, 1H, NH), 13.79 (bs, 1H, COOH); ^{13}C NMR (101 MHz, DMSO- d_6): δ 16.9, 108.8, 116.9, 119.9, 123.5, 127.7, 129.1, 131.4, 131.6, 134.2, 135.8, 140.0, 149.1, 154.9, 157.3, 158.7, 161.3, 169.1. HRMS: m/z calcd for C₂₀H₁₅N₅O₃ 374.1275 (M + H⁺), found 374.1258 (M + H⁺). HPLC, ret. time: 4.48 min, peak area: 98.21%.

4.1.12. 2-(5-Methyl-7-phenyl-[1,2,4]triazolo[1,5-*a*]pyrimidin-2-yl)-4H-benzo[d][1,3]oxazin-4-one (**22**)

The title compound was prepared starting from **41** [19] and 2-

aminobenzoic acid by Method A and purified by crystallization by MeOH/DMF in 31% yield. ¹H NMR (400 MHz, CDCl₃): δ 2.82 (s, 3H, CH₃), 7.20 (s, 1H, H₆), 7.60–7.65 (m, 4H, Ar–H), 7.87–7.94 (m, 2H, Ar–H), 8.13–8.16 (m, 2H, Ar–H), 8.30 (d, *J* = 7.7 Hz, 1H, Ar–H); ¹³C NMR (101 MHz, DMSO-*d*₆): δ 25.7, 111.5, 118.1, 128.4, 128.9, 129.2, 129.3, 129.5, 129.7, 132.2, 136.8, 146.2, 147.7, 150.9, 156.8, 157.7, 158.5, 166.9. HRMS: *m/z* calcd for C₂₀H₁₃N₅O₂ 356.1154 (M + H⁺), found 356.1145 (M + H⁺). HPLC, ret. time: 3.78 min, peak area: 99.95%.

4.1.13. 2-(7-Methyl-5-phenyl-[1,2,4]triazolo[1,5-*a*]pyrimidin-2-yl)-4H-benzo[d][1,3]oxazin-4-one (**23**)

A mixture of **19** (0.06 g, 0.16 mmol) and acetic anhydride (0.016 g, 1.68 mmol) was heated at 100 °C overnight. After cooling, the reaction mixture was poured into ice/water obtaining a precipitate that was filtered and purified by flash chromatography eluting with 100% CHCl₃ to give **23** (0.026 g, 45% yield). ¹H NMR (400 MHz, CDCl₃): δ 3.02 (s, 3H, CH₃), 7.51–7.55 (m, 4H, Ar–H and H₆), 7.61–7.65 (m, 1H, Ar–H), 7.87–7.95 (m, 2H, Ar–H), 8.21–8.24 (m, 2H, Ar–H), 8.31 (d, *J* = 7.7 Hz, 1H, Ar–H); ¹³C NMR (101 MHz, CDCl₃): δ 17.8, 108.5, 118.1, 128.0, 128.4, 128.9, 129.2, 129.7, 131.8, 136.0, 136.9, 146.2, 148.1, 150.9, 156.2, 158.0, 158.4, 162.5. HRMS: *m/z* calcd for C₂₀H₁₃N₅O₂ 356.1158 (M + H⁺), found 356.1148 (M + H⁺). HPLC, ret. time: 2.95 min, peak area: 99.83%.

4.1.14. General procedure for the synthesis of compounds **24**–**27** by amidation (method B)

A solution of benzoyl chloride (2.0 mmol) in dry pyridine (5 mL) was added dropwise to a solution of the appropriate [1,2,4]triazolo[1,5-*a*]pyrimidine-2-amine (**8**–**11**) (1.0 mmol) in dry pyridine (15 mL), and then the reaction mixture was maintained at 80 °C until no starting material was detected by TLC. After cooling, it was poured into ice/water and acidified with CH₃COOH (pH = 5), obtaining a precipitate that was filtered and purified as described below.

4.1.15. *N*-(7-Phenyl-[1,2,4]triazolo[1,5-*a*]pyrimidin-2-yl)benzamide (**24**)

The title compound was prepared starting from **8** (4 h) by Method B and purified by flash chromatography eluting with CH₂Cl₂/MeOH (97:3) in 64% yield. ¹H NMR (400 MHz, DMSO-*d*₆): δ 7.49 (t, *J* = 7.8 Hz, 2H, Ar–H), 7.55–7.63 (m, 5H, H₆ and Ar–H), 7.99–8.00 (m, 2H, Ar–H), 8.21–8.23 (m, 2H, Ar–H), 8.83 (d, *J* = 4.8 Hz, 1H, H-5), 11.41 (s, 1H, NH); ¹³C NMR (101 MHz, DMSO-*d*₆): δ 109.7, 128.5, 128.8, 129.0, 129.9, 130.0, 132.0, 132.6, 133.9, 146.9, 154.7, 155.3, 160.5, 165.3. HRMS: *m/z* calcd for C₁₈H₁₃N₅O 316.1199 (M + H⁺), found 316.11978 (M + H⁺). HPLC, ret. time: 3.95 min, peak area: 100%.

4.1.16. *N*-(5-Phenyl-[1,2,4]triazolo[1,5-*a*]pyrimidin-2-yl)benzamide (**25**)

The title compound was prepared starting from **9** (24 h) by Method B and purified by flash chromatography eluting with CHCl₃/MeOH (99:1) in 35% yield. ¹H NMR (400 MHz, DMSO-*d*₆): δ 7.50 (t, *J* = 7.3 Hz, 2H, Ar–H), 7.55–7.61 (m, 4H, Ar–H), 7.90 (d, *J* = 7.1 Hz, 1H, H₆), 7.99 (d, *J* = 7.3 Hz, 2H, Ar–H), 8.24–8.27 (m, 2H, Ar–H), 9.38 (d, *J* = 7.1 Hz, 1H, H₇), 11.41 (s, 1H, NH); ¹³C NMR (101 MHz, DMSO-*d*₆): δ 107.6, 127.9, 128.5, 128.8, 129.5, 131.7, 132.5, 134.0, 136.3, 137.3, 154.2, 160.6, 161.2, 165.2. HRMS: *m/z* calcd for C₁₈H₁₃N₅O 316.1199 (M + H⁺), found 316.1195 (M + H⁺). HPLC, ret. time: 3.84 min, peak area: 99.57%.

4.1.17. *N*-(6-Phenyl-[1,2,4]triazolo[1,5-*a*]pyrimidin-2-yl)benzamide (**26**)

The title compound was prepared starting from **10** (5 h) by

Method B and purified by flash chromatography eluting with CHCl₃/MeOH (99:1) in 44% yield. ¹H NMR (400 MHz, DMSO-*d*₆): δ 7.44 (t, *J* = 7.4 Hz, 1H, Ar–H), 7.48–7.53 (m, 4H, Ar–H), 7.59 (t, *J* = 7.2 Hz, 1H, Ar–H), 7.84 (d, *J* = 7.7 Hz, 2H, Ar–H), 8.01 (d, *J* = 8.1 Hz, 2H, Ar–H), 9.16 (d, *J* = 2.3 Hz, 1H, H₇), 9.72 (d, *J* = 2.3 Hz, 1H, H₅), 11.45 (s, 1H, NH); ¹³C NMR (101 MHz, DMSO-*d*₆): 123.7, 127.4, 128.5, 128.8, 128.9, 129.6, 132.6, 133.3, 133.9, 134.0, 153.4, 154.3, 161.1, 165.1. HRMS: *m/z* calcd for C₁₈H₁₃N₅O 316.1199 (M + H⁺), found 316.1194 (M + H⁺). HPLC, ret. time: 3.82 min, peak area: 99.84%.

4.1.18. *N*-(7-Hydroxy-5-phenyl-[1,2,4]triazolo[1,5-*a*]pyrimidin-2-yl)benzamide (**27**)

The title compound was prepared starting from **11** (3 h) by Method B and purified by flash chromatography eluting with CHCl₃/MeOH (99:1) in 45% yield. ¹H NMR (400 MHz, DMSO-*d*₆): δ 6.31 (s, 1H, H₆), 7.47–7.49 (m, 5H, Ar–H), 7.57–7.60 (m, 1H, Ar–H), 7.92–7.98 (m, 4H, Ar–H), 11.44 (s, 1H, NH); ¹³C NMR (101 MHz, DMSO-*d*₆): δ 92.3, 127.6, 128.4, 128.8, 129.1, 130.6, 132.7, 133.6, 134.4, 137.3, 156.6, 157.0, 161.1, 165.7. HRMS: *m/z* calcd for C₁₈H₁₃N₅O₂ 332.1148 (M + H⁺), found 332.1179 (M + H⁺). HPLC, ret. time: 3.33 min, peak area: 95.21%.

4.1.19. 7-Phenyl-[1,2,4]triazolo[1,5-*a*]pyrimidine-2-carboxylic acid (**43**)

A mixture of **14** (1.2 g, 4.47 mmol) and NaOH (0.2 g, 5.82 mmol) in MeOH (25 mL) was refluxed for 4 h. After cooling, the reaction mixture was poured into ice/water and acidified with 2 N HCl obtaining a precipitate that was filtered and treated with Et₂O, to give **43** (0.85 g, 85%). ¹H NMR (400 MHz, DMSO-*d*₆): δ 7.61–7.67 (m, 4H, Ar–H and H₆), 8.10–8.12 (m, 2H, Ar–H), 8.99 (d, *J* = 4.5 Hz, 1H, H₅).

4.1.20. 6-Phenyl-[1,2,4]triazolo[1,5-*a*]pyrimidine-2-carboxylic acid (**44**)

The title compound was prepared starting from **16** following the same procedure as used for the synthesis of **43** (1 h) in 100% yield. ¹H NMR (400 MHz, DMSO-*d*₆): δ 7.44–7.48 (m, 1H, Ar–H), 7.53 (t, *J* = 7.4 Hz, 2H, Ar–H), 7.85 (d, *J* = 7.5 Hz, 2H, Ar–H), 9.34 (s, 1H, H₇), 9.80 (s, 1H, H₅), 13.86 (s, 1H, COOH).

4.1.21. *N*-(2-Carbamoylphenyl)-7-phenyl-[1,2,4]triazolo[1,5-*a*]pyrimidine-2-carboxamide (**28**)

The title compound was prepared starting from **43** and 2-aminobenzamide by Method A and purified by recrystallization from MeOH/DMF in 42% yield. ¹H NMR (400 MHz, DMSO-*d*₆): δ 7.19 (t, *J* = 7.2 Hz, 1H, Ar–H), 7.56 (t, *J* = 7.3 Hz, 1H, Ar–H), 7.65–7.67 (m, 3H, Ar–H), 7.72–7.74 (m, 2H, CONH₂ and Ar–H), 7.85 (d, *J* = 7.9 Hz, 1H, Ar–H), 8.25–8.28 (m, 2H, Ar–H), 8.31 (bs, 1H, CONH₂), 8.68 (d, *J* = 8.1 Hz, 1H, Ar–H), 9.02–9.03 (m, 1H, H₅), 13.22 (s, 1H, NH); ¹³C NMR (101 MHz, DMSO-*d*₆): δ 110.9, 120.3, 120.5, 123.3, 128.7, 128.8, 129.1, 129.7, 131.9, 132.3, 136.6, 147.8, 155.9, 156.4, 157.1, 158.7, 170.4. HRMS: *m/z* calcd for C₁₉H₁₄N₆O₂ 359.1270 (M + H⁺), found 359.1257 (M + H⁺). HPLC, ret. time: 2.23 min, peak area: 99.14%.

4.1.22. *N*-(2-Carbamoylphenyl)-6-phenyl-[1,2,4]triazolo[1,5-*a*]pyrimidine-2-carboxamide (**29**)

The title compound was prepared starting from **44** and 2-aminobenzamide by Method A and purified by flash chromatography eluting with CHCl₃/MeOH (98:2), in 38% yield. ¹H NMR (400 MHz, DMSO-*d*₆): δ 7.20 (t, *J* = 7.6 Hz, 1H, Ar–H), 7.47 (t, *J* = 7.3 Hz, 1H, Ar–H), 7.52–7.58 (m, 3H, Ar–H), 7.75 (s, 1H, CONH₂), 7.84 (d, *J* = 7.8 Hz, 1H, Ar–H), 7.89 (d, *J* = 7.6 Hz, 2H, Ar–H), 8.33 (s, 1H, CONH₂), 8.70 (d, *J* = 8.3 Hz, 1H, Ar–H), 9.16 (d, *J* = 2.2 Hz, 1H, H₇), 9.86 (d, *J* = 2.1 Hz, 1H, H₅), 13.12 (s, 1H, NH); ¹³C NMR

(101 MHz, DMSO- d_6): δ 120.8, 121.0, 123.7, 125.5, 127.7, 129.1, 129.3, 129.7, 132.7, 132.8, 134.9, 138.9, 154.3, 156.7, 157.3, 159.7, 170.7. HRMS: m/z calcd for $C_{19}H_{14}N_6O_2$ 359.1257 ($M + H^+$), found 359.1236 ($M + H^+$). HPLC, ret. time: 3.89 min, peak area: 100%.

4.1.23. *N*-(3-Carbamoyl-5,6,7,8-tetrahydro-4H-cyclohepta[b]thiophen-2-yl)-7-phenyl-[1,2,4]triazolo[1,5-*a*]pyrimidine-2-carboxamide (**30**)

The title compound was prepared starting from **43** and 2-amino-5,6,7,8-tetrahydro-4H-cyclohepta[b]thiophene-3-carboxamide [**39**] by Method A and purified by flash chromatography eluting with $CHCl_3/MeOH$ (99:1) in 16% yield. 1H NMR (400 MHz, $CDCl_3$): δ 1.66–1.73 (m, 4H, cycloheptane $CH_2 \times 2$), 1.86–1.90 (m, 2H, cycloheptane CH_2), 2.76–2.80 (m, 4H, cycloheptane $CH_2 \times 2$), 7.39 (d, $J = 4.5$ Hz, 1H, H6), 7.60–7.66 (m, 3H, Ar-H), 8.15–8.18 (m, 2H, Ar-H), 9.00 (d, $J = 4.5$ Hz, 1H, H5), 10.14 (s, 1H, NH); ^{13}C NMR (101 MHz, $CDCl_3$): δ 26.4, 27.1, 28.2, 28.4, 31.1, 97.1, 109.6, 113.3, 127.9, 128.3, 128.7, 131.6, 132.4, 135.6, 141.8, 148.4, 154.4, 155.2, 155.3, 156.7. HRMS: m/z calcd for $C_{22}H_{20}N_6O_2S$ 437.1118 ($M + Na^+$)+[$-H_2O$], found 437.1162 ($M + Na^+$)+[$-H_2O$]. HPLC, ret. time: 4.78 min, peak area: 97.82%

4.1.24. *N*-(3-Carbamoyl-5,6,7,8-tetrahydro-4H-cyclohepta[b]thiophen-2-yl)-6-phenyl-[1,2,4]triazolo[1,5-*a*]pyrimidine-2-carboxamide (**31**)

The title compound was prepared starting from **44** and 2-amino-5,6,7,8-tetrahydro-4H-cyclohepta[b]thiophene-3-carboxamide [**39**] by Method A and purified by flash chromatography eluting with $CHCl_3/MeOH$ (95:5), in 42% yield. 1H NMR (400 MHz, DMSO- d_6): δ 1.58–1.59 (m, 4H, cycloheptane $CH_2 \times 2$), 1.77–1.79 (m, 2H, cycloheptane CH_2), 2.71–2.73 (m, 2H, cycloheptane CH_2), 2.79–2.85 (m, 2H, cycloheptane CH_2), 7.45–7.49 (m, 2H, Ar-H and CONH), 7.52–7.56 (m, 2H, Ar-H), 7.72 (bs, 1H, CONH), 7.88 (d, $J = 7.6$ Hz, 2H, Ar-H), 9.40 (d, $J = 1.9$ Hz, 1H, H7), 9.88 (d, $J = 1.8$ Hz, 1H, H5), 12.07 (s, 1H, NH); ^{13}C NMR (101 MHz, DMSO- d_6): δ 27.5, 27.9, 28.5, 28.7, 31.9, 122.1, 125.6, 127.7, 129.4, 129.7, 131.7, 132.7, 135.0, 135.5, 136.6, 154.2, 155.2, 156.9, 158.2, 167.7. HRMS: m/z calcd for $C_{22}H_{20}N_6O_2S$ 455.1266 ($M + Na^+$), found 455.12613 ($M + Na^+$). HPLC, ret. time: 5.071 min, peak area: 100%.

4.1.25. *N*-(2-Fluorophenyl)-7-methyl-5-phenyl-[1,2,4]triazolo[1,5-*a*]pyrimidine-2-carboxamide (**49**)

The title compound was prepared starting from **42** [**19**] and *o*-fluoroaniline by Method A and purified by flash chromatography eluting with CH_2Cl_2 , in 45% yield. 1H NMR (400 MHz, $CDCl_3$): δ 2.81 (s, 3H, CH_3), 7.17–7.28 and 7.53–7.61 (m, each 3H, Ar-H), 7.77 (t, $J = 7.3$ Hz, 1H, Ar-H), 8.11 (s, 1H, H-6), 8.23–8.27 (m, 2H, Ar-H), 10.48 (s, 1H, NH); ^{13}C NMR (101 MHz, $CDCl_3$): δ 17.47, 109.33, 116.26 ($J = 19.4$ Hz), 125.06, 127.77 ($J = 19.4$ Hz), 125.79, 127.26, 128.26, 129.70, 132.14, 136.47, 149.77, 155.31 ($J = 247.5$ Hz), 155.45, 158.02, 159.21, 162.04. HRMS: m/z calcd for $C_{19}H_{14}FN_5O$ 348.1261 ($M + H^+$), found 348.1263 ($M + H^+$). HPLC, Xterra C18; CH_3CN 80%: H_2O 20%; ret. time: 2.18 min, peak area: 96.59%.

4.2. Biology (IAV)

4.2.1. Compounds and peptide

RBV (1- β -ribofuranosyl-1,2,4-triazole-3-carboxamide) was purchased from Roche. Each test compound was dissolved in 100% DMSO. The PB1_(1–15)-Tat peptide was synthesized and purified by the Peptide Facility of CRIBI Biotechnology Center (University of Padua, Padua, Italy). This peptide corresponds to the first 15 amino acids of PB1 protein fused to a short sequence of HIV Tat protein (amino acids 47–59), which allows the delivery into the cell [**40**].

4.2.2. Cells and virus

Madin-Darby canine kidney (MDCK) cells were grown in Dulbecco's modified Eagle's medium (DMEM, Life Technologies) supplemented with 10% (v/v) fetal bovine serum (FBS, Life Technologies) and antibiotics (100 U/mL penicillin and 100 μ g/mL streptomycin, Life Technologies). Cells were maintained at 37 °C in a humidified atmosphere with 5% CO_2 . IAV A/PR/8/34 (H1N1, Cambridge lineage) was kindly provided by P. Digard (Roslin Institute, University of Edinburgh, United Kingdom).

4.2.3. PA-PB1 interaction enzyme-linked immunosorbent assay (ELISA)

The PA–PB1 interaction was detected by a procedure previously described [**17**]. Briefly, 96-well microtiter plates (Nuova Aptaca) were coated with 400 ng of 6His-PA_(239–716) for 3h at 37 °C and then blocked with 2% BSA (Sigma) in PBS for 1h at 37 °C. The 6His-PA_(239–716) protein was expressed in *E. coli* strain BL21(DE3)pLysS and purified as already described [**17**]. After washing, 200 ng of GST-PB1_(1–25), or of GST alone as a control, in the absence or the presence of test compounds at various concentrations, were added and incubated O/N at room temperature. *Escherichia coli*-expressed, purified GST and GST-PB1_(1–25) proteins were obtained as previously described [**17,41**]. After washing, the interaction between 6His-PA_(239–716) and GST-PB1_(1–25) was detected with a horseradish peroxidase-coupled anti-GST monoclonal antibody (GenScript) diluted 1:4000 in PBS supplemented with 2% FBS. Following washes, the substrate 3,3',5,5'-tetramethylbenzidine (TMB, KPL) was added and absorbance was measured at 450 nm by an ELISA plate reader (Tecan Sunrise™). Values obtained from the samples treated with only DMSO were set as 100% of PA–PB1 interaction.

4.2.4. Cytotoxicity assay

Cytotoxicity of compounds was tested in MDCK cells by the 3-(4,5-dimethylthiazol-2-yl)-2,5-diphenyl tetrazolium bromide (MTT) method, as previously reported [**17,42**]. Briefly, MDCK cells (seeded at density of 2×10^4 per well) were grown in 96-well plates for 24h and then treated with serial dilutions of test compounds, or DMSO as a control, in DMEM supplemented with 10% FBS. After incubation at 37 °C for 48h, 5 mg/mL of MTT (Sigma) in PBS was added into each well and incubated at 37 °C for further 4h. Successively, a solubilization solution (10% SDS, 0.01 N HCl) was added to lyse the cells and incubated O/N at 37 °C. Finally, optical density was read at the wavelength of 620 nm on a microtiter plate reader (Tecan Sunrise™).

4.2.5. Plaque reduction assay (PRA)

The antiviral activity of test compounds against IAV was tested by PRA as previously described [**17,43**]. MDCK cells were seeded at 5×10^5 cells/well into 12-well plates, and incubated at 37 °C for 24h. The following day, the culture medium was removed and the monolayers were first washed with serum-free DMEM and then infected with the IAV A/PR/8/34 strain at 40 PFU/well in DMEM supplemented with 1 μ g/mL of TPCK-treated trypsin (Worthington Biochemical Corporation) and 0.14% BSA and incubated for 1 h at 37 °C. The IAV infection was performed in the presence of different concentrations of test compounds or solvent (DMSO) as a control. After virus adsorption, DMEM containing 1 μ g/mL of TPCK-treated trypsin, 0.14% BSA, 1.2% Avicel, and DMSO or test compounds was added to the cells. At 48 h post-infection, cells were fixed with 4% formaldehyde and stained with 0.1% toluidine blue. Viral plaques were counted, and the mean plaque number in the DMSO-treated control was set at 100%.

4.2.6. Minireplicon assays

The minireplicon assay was performed as described [**17**], with

some modifications. Briefly, HEK 293T cells (2×10^5 cells per well) were plated into 24-well plates and incubated overnight at 37 °C. The next day, cells were transfected using calcium phosphate coprecipitation method with pcDNA-PB1, pcDNA-PB2, pcDNA-PA, pcDNA-NP plasmids (100 ng/well of each) along with 50 ng/well of the pPoll-Flu-ffLuc reporter plasmid and 50 ng/well of pRL-SV40 plasmid as a transfection control. Transfections were performed in the presence of different concentrations of test compounds or DMSO. RBV was used as a positive control for inhibition. Cell medium was removed 5 h post-transfection and replaced with DMEM containing the compounds, RBV, or DMSO. At 24 h post-transfection, cells were harvested, lysed and both firefly and *Renilla* luciferase activity were measured using the Dual Luciferase Assay Kit (Promega). In each experiment, firefly luciferase activity was normalized with that of the *Renilla* luciferase and relative luciferase units (RLU) were obtained. The activity measured in control transfection reactions containing DMSO was set at 100% of polymerase activity.

4.3. Biology (SARS-CoV-2)

4.3.1. Cells and viruses

The SARS-CoV-2 isolate used in this study was the BetaCov/Belgium/GHB-03021/2020 (EPI_ISL407976|2020-02-03), which was isolated from a Belgian patient returning from Wuhan in February 2020. The isolate was passaged 7 times on Vero E6 cells which introduced two series of amino acid deletions in the spike protein [44]. The infectious content of the virus stock was determined by titration on Vero E6 cells. Vero E6 cells were maintained in Dulbecco's modified Eagle's medium (DMEM; Gibco) supplemented with heat-inactivated 10% v/v fetal calf serum (FCS; Biowest) and 500 µg/mL Geneticin (Gibco) and kept under 5% CO₂ at 37 °C. All SARS-CoV-2-related experimental work was performed in the certified, high-containment biosafety level-3 facilities of the Rega Institute at the KU Leuven (Belgium).

4.3.2. SARS-CoV-2 screening

The SARS-CoV-2 antiviral assay is derived from the previously established SARS-CoV assay [45]. In this assay, fluorescence of Vero E6-eGFP cells (provided by Dr. K. Andries J&JPRD; Beerse, Belgium) declines after infection with SARS-CoV-2 due to the cytopathogenic effect of the virus. In the presence of an antiviral compound, the cytopathogenicity is inhibited and the fluorescent signal rescued. Stock solutions of the various compounds in DMSO (10 mM) were prepared. On day -1, the test compounds were serially diluted in assay medium (DMEM supplemented with 2% v/v FCS). The plates were incubated (37 °C, 5% CO₂ and 95% relative humidity) overnight. On day 0, the diluted compounds were then mixed with SARS-CoV-2 at 20 TCID₅₀/well and Vero E6-eGFP cells corresponding to a final density of 25,000 cells/well in 96-well black-view plates (Greiner Bio-One, Vilvoorde, Belgium). The plates were incubated in a humidified incubator at 37 °C and 5% CO₂. At 4 days p.i., the wells were examined for eGFP expression using an argon laser-scanning microscope. The microscope settings were excitation at 488 nm and emission at 510 nm and the fluorescence images of the wells were converted into signal values. The results were expressed as EC₅₀ values defined as the concentration of compound achieving 50% rescue of the virus-reduced eGFP signals as compared to the untreated virus-infected control cells. Toxicity of compounds in the absence of virus was evaluated in a standard MTS-assay as described previously [46].

Declaration of competing interest

The authors declare that they have no known competing

financial interests or personal relationships that could have appeared to influence the work reported in this paper.

Acknowledgements

This work was supported by grants "Excellent Departments" by Ministero dell'Istruzione, dell'Università e della Ricerca-MIUR (to S. Massari), PRIN 2017 - cod. 2017BMK8JR (to S. Massari, T. Felicetti and V. Cecchetti), Fondazione Cassa Risparmio Perugia - Ricerca Scientifica e Tecnologica 2019: "Giovani ricercatori: risorsa per il territorio" - cod. 3FCRPG19_SM (to M.C. Pismataro), Associazione Italiana per la Ricerca sul Cancro, AIRC, grant n. IG18855 (to A. Loregian); British Society for Antimicrobial Chemotherapy, UK, BSAC-2018-0064 (to A. Loregian), Ministero dell'Istruzione, dell'Università e della Ricerca, PRIN 2017 - cod. 2017KM79NN (to A. Loregian), Fondazione Cassa di Risparmio di Padova e Rovigo - Bando Ricerca Covid-2019 Nr. 55777 2020.0162 (to A. Loregian). The SARS-CoV-2 research was performed using the 'Caps-It' research infrastructure (project ZW13-02) that was financially supported by the Hercules Foundation and Rega Foundation, KU Leuven.

Appendix A. Supplementary data

Supplementary data to this article can be found online at <https://doi.org/10.1016/j.ejmech.2021.113494>.

References

- [1] Antiviral agents for the treatment and chemoprophylaxis of influenza, *Ann. Emerg. Med.* 58 (2011) 299–303. <https://www.cdc.gov/mmwr/preview/mmwrhtml/rr6001a1.htm>.
- [2] M.G. Ison, Antiviral treatments, *Clin. Chest Med.* 38 (2017) 139–153. <https://doi.org/10.1016/j.ccm.2016.11.008>.
- [3] L.V. Gubareva, L. Kaiser, F.G. Hayden, Influenza virus neuraminidase inhibitors, *Lancet* 355 (2000) 827–835. [https://doi.org/10.1016/S0140-6736\(99\)11433-8](https://doi.org/10.1016/S0140-6736(99)11433-8).
- [4] J.M. Wandzik, T. Kouba, S. Cusack, Structure and function of influenza polymerase, *Cold Spring Harb. Perspect. Med.* (2020) a038372. <https://doi.org/10.1101/cshperspect.a038372>.
- [5] E. Fodor, A.J.W.T. Velthuis, Structure and function of the influenza virus transcription and replication machinery, *Cold Spring Harb. Perspect. Med.* 10 (2020) 1–14. <https://doi.org/10.1101/cshperspect.a038398>.
- [6] E.J. Mifsud, F.G. Hayden, A.C. Hurt, Antivirals targeting the polymerase complex of influenza viruses, *Antivir. Res.* 169 (2019) 104545. <https://doi.org/10.1016/j.antiviral.2019.104545>.
- [7] J. Zhang, Y. Hu, R. Musharrafieh, H. Yin, J. Wang, Focusing on the influenza virus polymerase complex: recent progress in drug discovery and assay development, *Curr. Med. Chem.* 26 (2018) 2243–2263. <https://doi.org/10.2174/0929867325666180706112940>.
- [8] I. Giacchello, F. Musumeci, I. D'Agostino, C. Greco, G. Grossi, S. Schenone, Insights into RNA-dependent RNA polymerase inhibitors as anti-influenza virus agents, *Curr. Med. Chem.* 27 (2020). <https://doi.org/10.2174/0929867327666200114115632>.
- [9] M. Toots, R.K. Plempner, Next-generation direct-acting influenza therapeutics, *Transl. Res.* 220 (2020) 33–42. <https://doi.org/10.1016/j.trsl.2020.01.005>.
- [10] Y. Furuta, K. Takahashi, Y. Fukuda, M. Kuno, T. Kamiyama, K. Kozaki, N. Nomura, H. Egawa, S. Minami, Y. Watanabe, H. Narita, K. Shiraki, In vitro and in vivo activities of anti-influenza virus compound T-705, *Antimicrob. Agents Chemother.* 46 (2002) 977–981.
- [11] Y. Furuta, B.B. Gowen, K. Takahashi, K. Shiraki, D.F. Smee, D.L. Barnard, Favipiravir (T-705), a novel viral RNA polymerase inhibitor, *Antivir. Res.* 100 (2013) 446–454. <https://doi.org/10.1016/j.antiviral.2013.09.015>.
- [12] J.C. Jones, B.M. Marathe, C. Lerner, L. Kreis, R. Gasser, P.N.Q. Pascua, I. Najera, E.A. Govorkova, A novel endonuclease inhibitor exhibits broad-spectrum anti-influenza virus activity in Vitro, *Antimicrob. Agents Chemother.* 60 (2016) 5504–5514. <https://doi.org/10.1128/AAC.00888-16>.
- [13] T. Noshi, M. Kitano, K. Taniguchi, A. Yamamoto, S. Omoto, K. Baba, T. Hashimoto, K. Ishida, Y. Kushima, K. Hattori, M. Kawai, R. Yoshida, M. Kobayashi, T. Yoshinaga, A. Sato, M. Okamatsu, Y. Sakoda, H. Kida, T. Shishido, A. Naito, In vitro characterization of baloxavir acid, a first-in-class cap-dependent endonuclease inhibitor of the influenza virus polymerase PA subunit, *Antivir. Res.* 160 (2018) 109–117. <https://doi.org/10.1016/j.antiviral.2018.10.008>.
- [14] M.P. Clark, M.W. Ledebner, I. Davies, R.A. Byrn, S.M. Jones, E. Perola, A. Tsai, M. Jacobs, K. Nti-Addae, U.K. Bandarage, M.J. Boyd, R.S. Bethiel, J.J. Court, H. Deng, J.P. Duffy, W.A. Dorsch, L.J. Farmer, H. Gao, W. Gu, K. Jackson, D.H. Jacobs, J.M. Kennedy, B. Ledford, J. Liang, F. Maltais, M. Murcko, T. Wang,

- M.W. Wannamaker, H.B. Bennett, J.R. Leeman, C. McNeil, W.P. Taylor, C. Memmott, M. Jiang, R. Rinjbrand, C. Bral, U. Germann, A. Nezami, Y. Zhang, F.G. Salituro, Y.L. Bennani, P.S. Charifson, Discovery of a novel, first-in-class, orally bioavailable azaindole inhibitor (VX-787) of influenza PB2, *J. Med. Chem.* 57 (2014) 6668–6678, <https://doi.org/10.1021/jm5007275>.
- [15] R.W. Finberg, R. Lanno, D. Anderson, R. Fleischhackl, W. Van Duijnoven, R.S. Kauffman, T. Kosoglou, J. Vingerhoets, L. Leopold, Phase 2b study of pimodivir (JNJ-63623872) as monotherapy or in combination with oseltamivir for treatment of acute uncomplicated seasonal influenza A: TOPAZ trial, *J. Infect. Dis.* 219 (2019) 1026–1034, <https://doi.org/10.1093/infdis/jiy547>.
- [16] Janssen, Janssen to Discontinue Pimodivir Influenza Development Program, Johnson & Johnson, 2020. <https://johnsonandjohnson.gcs-web.com/news-releases/news-release-details/janssen-discontinue-pimodivir-influenza-development-program>. (Accessed 28 March 2021).
- [17] G. Muratore, L. Goracci, B. Mercorelli, A. Foeglein, P. Digard, G. Cruciani, G. Palù, A. Loregian, Small molecule inhibitors of influenza A and B viruses that act by disrupting subunit interactions of the viral polymerase, *Proc. Natl. Acad. Sci. U. S. A.* 109 (2012) 6247–6252, <https://doi.org/10.1073/pnas.1119817109>.
- [18] S. Massari, G. Nannetti, L. Goracci, L. Sancineto, G. Muratore, S. Sabatini, G. Manfroni, B. Mercorelli, V. Cecchetti, M. Facchini, G. Palù, G. Cruciani, A. Loregian, O. Tabarrini, G. Palù, G. Cruciani, A. Loregian, O. Tabarrini, Structural investigation of cycloheptathiophene-3-carboxamide derivatives targeting influenza virus polymerase assembly, *J. Med. Chem.* 56 (2013) 10118–10131, <https://doi.org/10.1021/jm401560v>.
- [19] S. Massari, G. Nannetti, J. Desantis, G. Muratore, S. Sabatini, G. Manfroni, B. Mercorelli, V. Cecchetti, G. Palù, G. Cruciani, A. Loregian, L. Goracci, O. Tabarrini, A Broad anti-influenza hybrid small molecule that potently disrupts the interaction of polymerase acidic protein-basic protein 1 (PA-PB1) subunits, *J. Med. Chem.* 58 (2015) 3830–3842, <https://doi.org/10.1021/acs.jmedchem.5b00012>.
- [20] S. Massari, L. Goracci, J. Desantis, O. Tabarrini, Polymerase acidic protein-basic protein 1 (PA-PB1) protein-protein interaction as a target for next-generation anti-influenza therapeutics, *J. Med. Chem.* 59 (2016) 7699–7718, <https://doi.org/10.1021/acs.jmedchem.5b01474>.
- [21] S. Massari, J. Desantis, M.G. Nizi, V. Cecchetti, O. Tabarrini, Inhibition of influenza virus polymerase by interfering with its protein-protein interactions, *ACS Infect. Dis.* (2020), <https://doi.org/10.1021/acscinfed.0c00552>.
- [22] X. He, J. Zhou, M. Bartlam, R. Zhang, J. Ma, Z. Lou, X. Li, J. Li, A. Joachimiak, Z. Zeng, R. Ge, Z. Rao, Y. Liu, Crystal structure of the polymerase PAC–PB1N complex from an avian influenza H5N1 virus, *Nature* 454 (2008) 1123–1126, <https://doi.org/10.1038/nature07120>.
- [23] B. Mänz, V. Götz, K. Wunderlich, J. Eisel, J. Kirchmair, J. Stech, O. Stech, G. Chase, R. Frank, M. Schwemmler, Disruption of the viral polymerase complex assembly as a novel approach to attenuate influenza A virus, *J. Biol. Chem.* 286 (2011) 8414–8424.
- [24] S. Massari, C. Bertagnin, M.C. Pismataro, A. Donnadio, G. Nannetti, T. Felicetti, S. Di Bona, M.G. Nizi, L. Tensi, G. Manfroni, M.I. Loza, S. Sabatini, V. Cecchetti, J. Brea, L. Goracci, A. Loregian, O. Tabarrini, Synthesis and characterization of 1,2,4-triazolo[1,5-a]pyrimidine-2-carboxamide-based compounds targeting the PA-PB1 interface of influenza A virus polymerase, *Eur. J. Med. Chem.* 209 (2021) 112944, <https://doi.org/10.1016/j.ejmech.2020.112944>.
- [25] S. Massari, J. Desantis, G. Nannetti, S. Sabatini, S. Tortorella, L. Goracci, V. Cecchetti, A. Loregian, O. Tabarrini, Efficient and regioselective one-step synthesis of 7-aryl-5-methyl- and 5-aryl-7-methyl-2-amino-[1,2,4]triazolo[1,5-a]pyrimidine derivatives, *Org. Biomol. Chem.* 15 (2017) 7944–7955, <https://doi.org/10.1039/C7OB02085F>.
- [26] P.K. Singh, S. Choudhary, A. Kashyap, H. Verma, S. Kapil, M. Kumar, M. Arora, O. Silakari, An exhaustive compilation on chemistry of triazolopyrimidine: a journey through decades, *Bioorg. Chem.* 88 (2019) 102919, <https://doi.org/10.1016/j.bioorg.2019.102919>.
- [27] Q. Renyu, L. Yuchao, W.M.W.V. Kandegama, C. Qiong, Y. Guangfu, Recent applications of triazolopyrimidine-based bioactive compounds in medicinal and agrochemical chemistry, *Mini Rev. Med. Chem.* 18 (2018) 781–793, <https://doi.org/10.2174/138955751766617110112850>.
- [28] S.A. El-Sebaey, Recent advances in 1,2,4-triazole scaffolds as antiviral agents, *Chemistry 5* (2020) 11654–11680, <https://doi.org/10.1002/slct.202002830>.
- [29] C.J.A. Ribeiro, J. Kankanala, J. Xie, J. Williams, H. Aihara, Z. Wang, Triazolopyrimidine and triazolopyridine scaffolds as TDP2 inhibitors, *Bioorg. Med. Chem. Lett* 29 (2019) 257–261, <https://doi.org/10.1016/j.bmcl.2018.11.044>.
- [30] C.J. Menet, S.R. Fletcher, G. Van Lommen, R. Geney, J. Blanc, K. Smits, N. Jouannigot, P. Deprez, E.M. van der Aar, P. Clement-Lacroix, L. Lepescheux, R. Galien, B. Vayssiere, L. Nelles, T. Christophe, R. Brys, M. Uhring, F. Ciesielski, L. Van Rompaey, Triazolopyridines as selective JAK1 inhibitors: from hit identification to GLPG0634, *J. Med. Chem.* 57 (2014) 9323–9342, <https://doi.org/10.1021/jm501262q>.
- [31] J.C. Castillo, H.A. Rosero, J. Portilla, Simple access toward 3-halo- and 3-nitro-pyrazolo[1,5-a] pyrimidines through a one-pot sequence, *RSC Adv.* 7 (2017) 28483–28488, <https://doi.org/10.1039/c7ra04336h>.
- [32] F. Chung, C. Tisné, T. Lecourt, B. Seijo, F. Dardel, L. Micouin, Design of tRNA^{Lys3} Ligands: fragment evolution and linker selection guided by NMR spectroscopy, *Chem. Eur. J.* 15 (2009) 7108–7116, <https://doi.org/10.1002/chem.200802451>.
- [33] B.D. Alexander, J.A. Crayston, T.J. Dines, Cyclic voltammetry and spectroelectrochemical study of nickel and cobalt diphenyltetraazaannulene complexes, *J. Electroanal. Chem.* 605 (2007) 109–117, <https://doi.org/10.1016/j.jelechem.2007.03.026>.
- [34] L.A. Souza, J.M. Santos, M. Mittersteiner, V.P. Andrade, M.M. Lobo, F.B. Santos, A.J. Bortoluzzi, H.G. Bonacorso, M.A.P. Martins, N. Zanatta, Synthetic versatility of β-alkoxyvinyl trichloromethyl ketones for obtaining [1,2,4]Triazol[1,5-a] pyrimidines, *Synth. Met.* 50 (2018) 3686–3695, <https://doi.org/10.1055/s-0037-1610191>.
- [35] D.C. Schmitt, N. Niljianskul, N.W. Sach, J.I. Trujillo, A parallel approach to 7-(hetero)arylp[pyrazolo[1,5-a]pyrimidin-5-ones, *ACS Comb. Sci.* 20 (2018) 256–260, <https://doi.org/10.1021/acscombsci.8b00032>.
- [36] Y. Li, L. Cao, G. Li, F. Cong, Y. Li, J. Sun, Y. Luo, G. Chen, G. Li, P. Wang, F. Xing, Y. Ji, J. Zhao, Y. Zhang, D. Guo, X. Zhang, Remdesivir metabolite GS-441524 effectively inhibits SARS-CoV-2 infection in mouse models, *J. Med. Chem.* (2021), <https://doi.org/10.1021/acs.jmedchem.0c01929>.
- [37] J. Desantis, S. Massari, A. Corona, A. Astolfi, S. Sabatini, G. Manfroni, D. Palazzotti, V. Cecchetti, C. Pannecouque, E. Tramontano, O. Tabarrini, 1,2,4-Triazol[1,5-a]pyrimidines as a novel class of inhibitors of the HIV-1 reverse transcriptase-associated ribonuclease H activity, *Molecules* 25 (2020) 1183, <https://doi.org/10.3390/molecules25051183>.
- [38] V.M. Chernyshev, A.V. Chernysheva, V.A. Taranushchik, Synthesis of esters and amides of 5-amino-1,2,4-triazole-3-carboxylic and 5-amino-1,2,4-triazol-3-ylacetic acids, *Russ. J. Appl. Chem.* 79 (2006) 783–786, <https://doi.org/10.1134/S1070427206050168>.
- [39] Y.D. Wang, S. Johnson, D. Powell, J.P. McGinnis, M. Miranda, S.K. Rabindran, Inhibition of tumor cell proliferation by thieno[2,3-d]pyrimidin-4(1H)-one-based analogs, *Bioorg. Med. Chem. Lett* 15 (2005) 3763–3766, <https://doi.org/10.1016/j.bmcl.2005.05.127>.
- [40] S. Fawell, J. Seery, Y. Daikh, C. Moore, L.L. Chen, B. Pepinsky, J. Barsoum, Targeted delivery of heterologous proteins into cells, *Proc. Natl. Acad. Sci. U. S. A.* 91 (1994) 664–668.
- [41] A. Loregian, B.A. Appleton, J.M. Hogle, D.M. Coen, Residues of human cytomegalovirus DNA polymerase catalytic subunit UL54 that are necessary and sufficient for interaction with the accessory protein UL44, *J. Virol.* 78 (2004) 158–167, <https://doi.org/10.1128/jvi.78.1.158-167.2004>.
- [42] A. Loregian, D.M. Coen, Selective anti-cytomegalovirus compounds discovered by screening for inhibitors of subunit interactions of the viral polymerase, *Chem. Biol.* 13 (2006) 191–200, <https://doi.org/10.1016/j.chembiol.2005.12.002>.
- [43] G. Muratore, B. Mercorelli, L. Goracci, G. Cruciani, P. Digard, G. Palù, A. Loregian, Human cytomegalovirus inhibitor AL18 also possesses activity against influenza A and B viruses, *Antimicrob. Agents Chemother.* 56 (2012) 6009–6013, <https://doi.org/10.1128/AAC.01219-12>.
- [44] R. Boudewijns, H.J. Thibaut, S.J.F. Kaptein, R. Li, V. Vergote, L. Seldeslachts, J. Van Weyenbergh, C. De Keyzer, L. Bervoets, S. Sharma, L. Liesenborghs, J. Ma, S. Jansen, D. Van Looveren, T. Verduyssen, X. Wang, D. Jochmans, E. Martens, K. Roose, D. De Vlioger, B. Schepens, T. Van Buyten, S. Jacobs, Y. Liu, J. Martí-Carreras, B. Vanmechelen, T. Wawina-Bokalanga, L. Delang, J. Rocha-Pereira, L. Coelmont, W. Chiu, P. Leysen, E. Heylen, D. Schols, L. Wang, L. Close, J. Matthijnsens, M. Van Ranst, V. Compennolle, G. Schramm, K. Van Laere, X. Saelens, N. Callewaert, G. Opdenakker, P. Maes, B. Weynand, C. Cawthorne, G. Vande Velde, Z. Wang, J. Neyts, K. Dallmeier, STAT2 signaling restricts viral dissemination but drives severe pneumonia in SARS-CoV-2 infected hamsters, *Nat. Commun.* 11 (2020), <https://doi.org/10.1038/s41467-020-19684-y>.
- [45] T. Ivens, C. Van Den Eynde, K. Van Acker, E. Nijs, G. Dams, E. Bettens, A. Ohagen, R. Pauwels, K. Hertogs, Development of a homogeneous screening assay for automated detection of antiviral agents active against severe acute respiratory syndrome-associated coronavirus, *J. Virol. Methods.* 129 (2005) 56–63, <https://doi.org/10.1016/j.jviromet.2005.05.010>.
- [46] D. Jochmans, P. Leysen, J. Neyts, D. A. Jochmans, P. Leysen, J. Neyts, A novel method for high-throughput screening to quantify antiviral activity against viruses that induce limited CPE, *J. Virol. Methods* 183 (2) (2012) 176–179, <https://doi.org/10.1016/j.jviromet.2012.04.011>.